UNIVERSIDAD AUTÓNOMA METROPOLITANA

AZCAPOTZALCO

MASTER THESIS

SIMULATION OF THE SPATIAL Ca^{2+} DYNAMICS IN CARDIAC CELLS

Author:
Hugo Enrique ROMERO CAMPOS

Advisors:
Dr. Virginia GONZÁLEZ VÉLEZ
Profesora Investigadora, Departamento de Ciencias Básicas, (UAM-A), México
Dr. Geneviève DUPONT
Directrice de recherches FNRS, Faculté des Sciences (ULB), Belgium

Examiners:
Dr. Roberto Ávila Pozos (UAEH)
Dr. Daniel Olmos Liceaga (USON)
Dr. Cutberto José Juvencio Galíndez Mayer (IPN)
Dr. Virginia González Vélez (UAM-A)

A thesis submitted in fulfillment of the requirements
for the degree of Master in Process Engineering
in the
Master in Process Engineering
Division of Basic Sciences and Engineering

Azcapotzalco, Mexico City, March 15th, 2018

Universidad Autónoma Metropolitana Azcapotzalco

Abstract

UAM-Azcapotzalco
Division of Basic Sciences and Engineering

Master in Process Engineering

SIMULATION OF THE SPATIAL Ca^{2+} DYNAMICS IN CARDIAC CELLS

by Hugo Enrique ROMERO CAMPOS

It is well known that mitochondrial metabolism is linked to Ca^{2+} dynamics in a complex manner. This relation underlies on the capacity of mitochondria to uptake, release and storage Ca^{2+} as well as on the activation of the energetic metabolism by mitochondrial Ca^{2+}. In *cardiomyocytes* (cardiac cells) this interplay becomes very important because of both the high energy demand (tissue-characteristic) and the regulation of excitation-contraction coupling by Ca^{2+}. Ca^{2+} dynamics and mitochondrial metabolism has been defined as a key issue in cardiac physiology and pathology. However, experimental methods have strong limitations due to the difficulties in measuring dynamic mitochondrial Ca^{2+} in the intricated cellular structure of *cardiomyocytes*, leading to controversial experimental results.

In the present project the relationship between Ca^{2+} dynamics and mitochondrial metabolism was addressed by modelling and simulation approach. Since in *cardiomyocytes*, Ca^{2+} increases are highly heterogeneous due to the cell structure, spatial aspects are considered as a main aspect. In fact, the working hypothesis is that the location of mitochondria with respect to Ca^{2+} channels plays a crucial role in determining the kinetics of Ca^{2+} changes and metabolism.

As a first step, a previous model that properly describes the coupling between Ca^{2+} signalling and mitochondrial metabolism in a non-excitable cells (Wacquier et al., 2016) was used as a base to develop a new mitochondrial model (MM) able to account for the particular features of mitochondria in cardiac cells.

In a second step, a compartmental modelling approach was used to account for the spatial aspects, so a coupled model (CM) was developed with the MM inside a model of a human ventricular *myocyte* (Grandi, Pasqualini, and Bers, 2010).

Finally, the whole new model was used to prove that mitochondrial position has significant effect on Ca^{2+} dynamics and mitochondrial metabolism through the design of three scenarios corresponding to particular distributions and interactions between mitochondria and other intracellular compartments of the cardiac cell model.

Universidad Autónoma Metropolitana Azcapotzalco

Resumen

UAM-Azcapotzalco
División de Ciencias Básicas e Ingeniería
Maestría en Ingeniería de Procesos

SIMULACIÓN DE LA DINÁMICA ESPACIAL DE Ca^{2+} EN CÉLULAS CARDIACAS

por Hugo Enrique ROMERO CAMPOS

En años recientes se ha verificado que el metabolismo mitocondrial y la dinámica de Ca^{2+} se encuentran acoplados de forma compleja, lo cual se debe a la capacidad de la mitocondria de captar, almacenar y liberar iones Ca^{2+}, así como a la activación del metabolismo energético por el Ca^{2+} mitocondrial. En los cardiomiocitos (células cardiacas), la alta demanda energética y la regulación del Ca^{2+} sobre el acople excitación-contracción, vuelven determinante la interrelación entre los procesos antes mencionados. Incluso, el problema de la dinámica de Ca^{2+} y el metabolismo mitocondrial se ha definido como uno de los campos centrales en la fisiología y patología cardiacas. En este sentido, los métodos experimentales han enfrentado grandes dificultades para medir Ca^{2+} mitocondrial dinámico dentro de la estructura celular de los cardiomiocitos, lo que ha llevado a resultados experimentales controversiales.

En el presente trabajo, la relación entre la dinámica de Ca^{2+} y el metabolismo mitocondrial se abordó mediante un enfoque de modelado y simulación. Además, dado que los cardiomiocitos presentan incrementos de Ca^{2+} altamente heterogéneos, por su estructura celular, la investigación se centró en el aspecto espacial. Así, la hipótesis de investigación es que, en los miocitos cardiacos, la localización de la mitocondria con respecto al espacio diádico determina los cambios en la dinámica de calcio y el metabolismo mitocondrial.

En una primera etapa, se utilizó un modelo recientemente publicado (Wacquier et al., 2016) que describe la interrelación entre la señalización del Ca^{2+} y el metabolismo mitocondrial en células no excitables para desarrollar un modelo mitocondrial (MM) capaz de reproducir las características particulares de la mitocondria en las células cardiacas.

En la segunda etapa se utilizó un enfoque de modelado compartamental con el fin de tomar en cuenta los aspectos espaciales, y se obtuvo un modelo acoplado (CM) integrado por el MM y un modelo de miocito ventricular humano (Grandi, Pasqualini, and Bers, 2010).

Finalmente, el nuevo modelo integral se utilizó para demostrar que la posición de la mitocondria tiene un efecto significativo en la dinámica del Ca^{2+} y el metabolismo mitocondrial, lo anterior se realizó mediante el análisis de tres escenarios que corresponden distribuciones e interacciones particulares entre la mitocondria y los compartimentos intracelulares del modelo de célula cardiaca.

Contents

List of Figures

List of Tables

Acknowledgements

- *This work could not have been possible without the direction and support of Virginia González Vélez and Geneviève Dupont, thank you very much to both.*
- *To all my family and the closer people to me, Victor Romero, Elizabeth Campos, and Laura Romero, thank you for always support me in all personal issues.*
- *To Consejo Nacional de Ciencia y Tecnología (CONACyT), Mexico, for providing the Master scholarship and the financial support for a research stay through the Bilateral Cooperation Project (México-Bélgica).*

Chapter 1

Introduction

1.1 Importance of Ca^{2+} in cardiac cells

Calcium ion (Ca^{2+}) is one of the most important intracellular messengers in mammalians because it controls vital physiological functions such as secretion, contraction, transcription and metabolism. This is possible because of its physical and chemical properties that make it an excellent ligand of several intracellular receptors (mostly proteins). Moreover, it possess more sensitivity to spatial and temporal changes in concentration than other ions in the body (Na^+, K^+, Mg^{2+}) (Fedrizzi, Lim, and Carafoli, 2008; Blaustein, 1985; Bootman, Lipp, and Berridge, 2001).

A cell type in which Ca^{2+} has a key role is the cardiac cell (*myocyte*), which is the specialized muscle cell of the heart. The internal structure of *myocytes* is analogue to the skeletal muscle, that is, it contains contractile units denominated sarcomeres, which are constituted by specialized proteins such as actin, myosin, tropomyosin, and troponin. The interaction between the first two is the base of the contraction, while the latter two are responsible of the regulation of this phenomenon. Particularly, contraction occurs when there is an increase in cytosolic Ca^{2+} which binds to troponin, generating a conformational change in this protein, and consequently in tropomyosin. This leads to contraction via coupling of actin and myosin filaments (Barnett, 2005; Klabunde, 2007).

The process involving the increase in cytosolic Ca^{2+} and the consequent contraction is denominated Excitation-Contraction Coupling (ECC). The term excitation refers to an external stimulus that leads to the increase of intracellular Ca^{2+} concentration. In the case of *myocytes*, the stimulus is an action potential[1] coming from the sinoatrial nodule (Bakker and Rijen, 2010; Laske and Iaizzo, 2005). Once Ca^{2+} ions enter into the *myocyte*, several regulation mechanisms generate a highly-organized temporal and spatial distribution of Ca^{2+}. Some examples of these mechanisms are channels, exchangers and pumps. In *myocytes*, the interaction between the ECC and the mitochondrial function is vital for the proper functioning of the heart (Kohlhaas and Maack, 2013; Maack and O'Rourke, 2007).

In cardiac *myocytes*, the cytosol surrounds the contractile units which occupy the major part of cardiac muscle. Moreover, the cellular membrane folds inside these fibres as T tubules (transversal tubules), which permit an effective interaction between

[1] This action potential (AP) is also called electric pulse, and is a wave of electrical discharge that travels along the cell membrane modifying the distribution of electric charges.

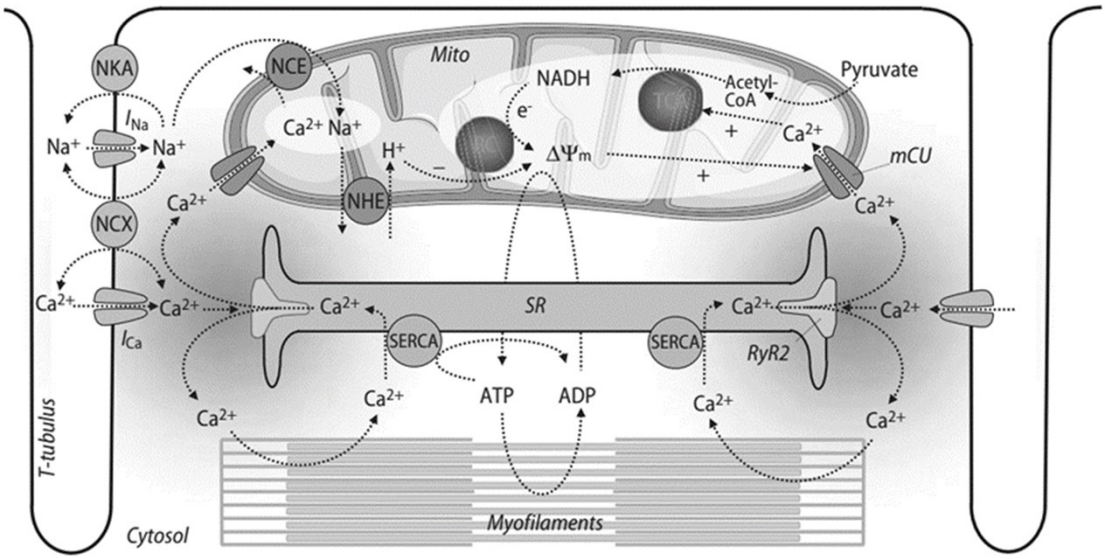

FIGURE 1.1: Regulation mechanisms of intracellular Ca^{2+} in excitation-contraction coupling and mitochondrial energy metabolism. *SR*, sarcoplasmic reticulum; *SERCA*, SR Ca^{2+} ATPase; *Mito*, mitochondria; *TCA*, tricarboxylic acid cycle; *RC*, respiratory chain; $\Delta\Psi_m$, mitochondrial membrane potential; *NCE*, mitochondrial Na^+/Ca^{2+}-exchanger; *NHE*, mitochondrial Na^+/H^+-exchanger; *NKA*, sarcolemmal Na^+/K^+-ATPase; *NCX*, sarcolemmal Na^+/Ca^{2+}-exchanger; *RyR2*, ryanodine receptor type 2; *mCU*, mitochondrial Ca^{2+} uniporter; I_{Na} and I_{Ca}, currents of voltage gated Na^+ and Ca^{2+}-channels, respectively (Maack and O'Rourke, 2007).

extracellular space and cytosol (Barnett, 2005; Bers, 2002). The regulation of ECC and mitochondrial metabolism by the Ca^{2+} transport mechanisms in a region close to the T tubule, is illustrated in Figure 1.1. ECC and mitochondrial metabolism are coupled for two reasons. The first reason is that both are regulated by the temporal and spatial dynamics of Ca^{2+}, in particular, mitochondria possess mechanisms to uptake and release Ca^{2+}, and it also works as a store of this ion (similar to endoplasmic reticulum), so that these facts modify the cytosolic Ca^{2+} dynamics (Dedkova and Blatter, 2013). The second reason is that the high energy demand of ECC as ATP, is supplied primarily by oxidative phosphorylation[2] which is a mitochondrial inherent process. It is important to note that mitochondrial Ca^{2+} dynamics stimulates ATP synthesis via activation of ATP synthase and some key dehydrogenases in Krebs cycle (Bers, 2008; Maack and O'Rourke, 2007).

Although the study of the system described above is feasible by experimental methods, a modelling and simulation approach is particularly useful and interesting for several reasons: it allows to analyse the parts of the system which contribute to a specific response of interest; it permits to elucidate underlying phenomena that experimental

[2]ATP (adenosine triphosphate) synthesis from ADP (adenosine diphosphate) and Pi (inorganic phosphorus) coupled with electron transfer from the reduced equivalents NADH and $FADH_2$ obtained in glycolysis and Krebs cycle.

data do not explicitly show; and it enables to propose and verify hypotheses which using experimental methods would be impossible or very expensive. In the same vein, it is important to recognize that a modelling and simulation approach does not exclude the experimental part, but on the contrary, uses it to verify whether the model reflects the known experimental facts and to prove which model improves the consistency of such observations (Kell and Knowles, 2006; Wolkenhauer, 2014).

1.2 The reaction-diffusion approach

Ca^{2+} dynamics can be modelled as a reactive system or as a reaction-diffusion system. In any case, stiff mathematical models are obtained because of the regulating and feedback mechanisms of Ca^{2+} and some other parts of the system. The contrast between the two system models is clear when it is noted that, the first assume spatial homogeneity, while the second takes into account the inherent heterogeneity of the system. In mathematical terms, the modelling of reactive systems leads to a nonlinear system of ordinary differential equations, while the modelling of reaction-diffusion systems leads to a nonlinear system of partial differential equations (Table 1.1) (Conrad and Tyson, 2006; Keener and Keizer, 2002).

TABLE 1.1: Two different approaches for Ca^{2+} dynamics modelling.

Approach	**Mathematical problem to solve**
Reactive System (time variable)	$accum. = input - output + generation - consumption$ Initial value problem $\frac{dX_i(t)}{dt} = F_i(X_1, X_2, \ldots, X_n, p_1, p_2, \ldots, p_m)\ ;\ i = 1, 2, \ldots, n$ With initial condition, $\{X_1(0), X_2(0), \ldots, X_n(0)\}$ Where $p_j\ ;\ j = 1, 2, \ldots, m$, are parameters of the model
Reaction-Diffusion System (space-time variables)	$accum. = diffusion + in. - out. + gen. - cons.$ Boundary value problem $\frac{\partial X_i(\mathbf{r},t)}{dt} = \nabla \cdot (D_i \nabla X_i) + F_i(X_1, X_2, \ldots, X_n, p_1, p_2, \ldots, p_m)$ With boundary cond. of Dirichlet, Neumann, etc. type Where p_j, are parameters of the model

The mathematical problems in Table 1.1 can be solved by analytical or numerical methods. However, the conditions under which analytical solutions are available are not common in models that represent cell regulation mechanisms. The complexity of the differential equation systems describing the temporal evolution and spatial distribution of Ca^{2+} is such that it is hard even using computational simulation studies (Conrad and Tyson, 2006). It is noteworthy that there is a wide range of computational software to implement models of reactive systems or reaction-diffusion systems for biological applications, some of which can be consulted in Szallasi, Stelling, and Periwal, 2006 and

in Ridgway, Broderick, and Ellison, 2006.

For cardiac *myocytes*, modelling studies need to make a balance between the necessity of a study of Ca^{2+} dynamics through the reaction-diffusion approach due to the great spatial heterogeneity generated by Ca^{2+} regulation mechanisms (Keener and Sneyd, 2008; Thul et al., 2015), and the costly computational work to solve the boundary value problem. For the purpose of this thesis, our interest is centred in the fact that the region of the steeper gradients and the dyadic cleft (in *myocytes*) can be properly modelled using a compartmental model, which in the field of Ca^{2+} modelling is referred as microdomains (Dupont et al., 2016; Hake and Lines, 2008).

1.3 Compartmental modelling

A compartmental model consists of interconnected chambers among which the interesting substances move. Also, it is assumed that the concentration of each specie is uniform within every compartment because of instant mixing (Enderle, 2011). Although this kind of models seem to be not very rigorous in describing realistic mechanistic features, it has been proved that they can be developed to levels (microdomains) to achieve it (Bassingthwaighte et al., 2012). In this regard, many successful works about modelling a ventricular *myocyte* underlie on that approach, which is also known as "common-pool" model (Winslow et al., 2011). As expected, compartmental models are reactive-like systems, because they lead to a nonlinear system of ordinary differential equations, but in contrast, the common-pool method takes spatial inhomogeneities into account and avoids having to simulate the very steep concentration gradients existing at the mouth of the Ca^{2+} channels, which are computationally very expensive, while providing a realist description of physiology (Dupont et al., 2016). In the present work, a compartmental model has been used to study the effect of mitochondrial position in determining the Ca^{2+} dynamics of ventricular *myocytes*.

Chapter 2

State of the art

2.1 Modelling intracellular Ca^{2+} dynamics and energy metabolism

Modelling Ca^{2+} dynamics began more than three decades ago with models whose aim was to reproduce and explain the oscillatory intracellular patterns of Ca^{2+} (Goldbeter, Dupont, and Berridge, 1990). At the beginning the "well-mixed cell models" were developed, where the cell is considered as a set of compartments representing organelles and cytosol within which the concentration of any specie is homogeneous. In this approach, Ca^{2+} fluxes through channels, pumps and exchangers, are described by empirical or semiempirical equations obtained via experimental kinetics (Keener and Sneyd, 2008).

The rapid development of experimental procedures to study molecular components of Ca^{2+} regulation mechanisms and the evident necessity of taking into account spatial heterogeneities in biological systems led to the construction of more complex models and to analyse the inherent reaction-diffusion process in these systems (Amundson and Clapham, 1993; Thul et al., 2008). Recently, the study of phenomena which are naturally coupled via Ca^{2+} signalling such as stimulus-secretion coupling, transcription regulation, excitation-contraction coupling, energy metabolism among others has been possible thanks to the high specialization of experimental methodologies and the possibility of solving more complex mathematical and computational models via computational implementation. Particularly, Winslow et al., 2011 presented a comprehensive review of the models that coupled processes like ECC and mitochondrial energy metabolism via Ca^{2+} dynamics in cardiac *myocytes*.

In recent years, it has been verified that mitochondrial metabolism is not coupled with Ca^{2+} dynamics in a simple manner, that is, it can greatly modify Ca^{2+} dynamics thanks to its capacity of uptake, release and storage of this ion (Rizzuto et al., 2012; Szabadkai and Duchen, 2008). On the other hand, studies of Ca^{2+} as an activator of energy metabolism in the ATP synthesis pathway have shown that it has a key role in the energy supply capacity of mitochondria (Denton, 2009; Griffiths and Rutter, 2009; Tarasov, Griffiths, and Rutter, 2012). Particularly, in cardiac *myocytes* the interplay between Ca^{2+} dynamics and mitochondrial metabolism becomes very important because of both, high energy demand and Ca^{2+} regulation of ECC. Even O'Rourke and Blatter, 2009 described the problem of Ca^{2+} dynamics and mitochondrial metabolism as a key issue in cardiac physiology and pathology, and they discussed how experimental methods utilized to

address the problem resulted in controversial data.

Based on the above description, modelling and simulation approaches arise as an alternative to elucidate the underlying mechanisms of Ca^{2+} dynamics and mitochondrial metabolism.

2.2 A mitochondrial model

The model reported by Wacquier et al., 2016 is able to reproduce the comprehensive Ca^{2+} dynamics within HeLa cells (Figure 2.1), focusing on the stimulation of mitochondrial metabolism by mitochondrial Ca^{2+}. Wacquier's model (WM) consists of seven ordinary differential equations for the concentration of cytosolic Ca^{2+} (Ca_c), mitochondrial Ca^{2+} (Ca_m), the fraction of inactivated IP_3 receptors (IP_3R), mitochondrial NADH (NADH), mitochondrial ADP (ADP_m), cytosolic ADP (ADP_c) and the mitochondrial membrane potential (MMP); and four conservation equations for the total Ca^{2+} in the cell, mitochondrial NADH, and the total adenine nucleotides in both mitochondria and cytosol (Table 2.1). These latter equations come from the fact that the system can be modelled as a closed system due to the short time scales investigated (Wacquier et al., 2016).

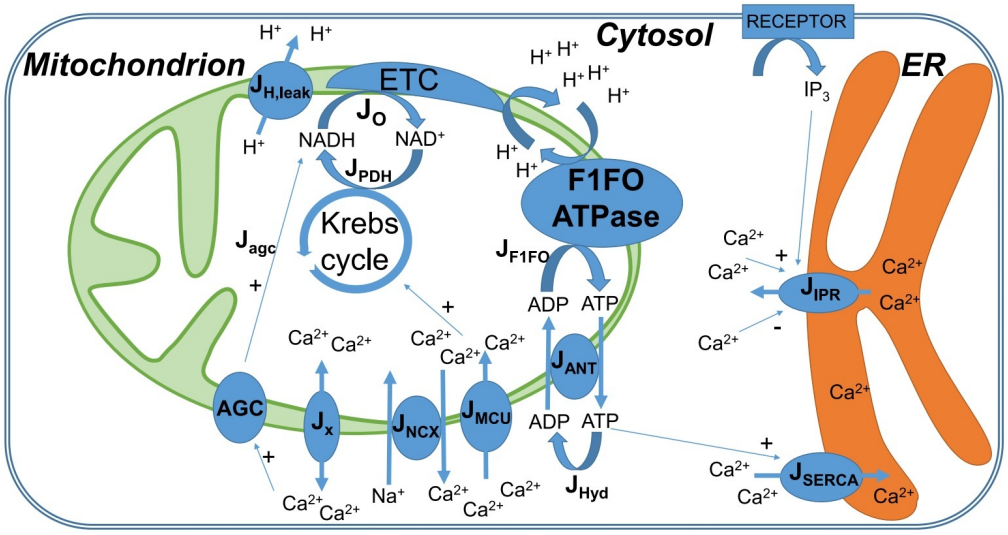

FIGURE 2.1: Schematic representation of mitochondrial model of Wacquier et al., 2016.

The full expression of the fluxes and the model parameters are in Appendix A. In Figure 2.2 are the Ca^{2+} dynamics in cytosol (c), endoplasmic reticulum (r) and mitochondria (m) simulated by WM under a stimulation by IP_3 (first 500 seconds) and without a stimulation (second 500 seconds).

TABLE 2.1: Dynamic and conservation equations of Wacquier's model.

Dynamic variable	Equation	Number
Dynamic equations		
Cytosolic Ca^{2+}	$\frac{dCa_c}{dt} = f_c(\alpha J_{IP3} - J_{SERCA} - \delta J_{MCU} + \delta J_{NCX} - \delta J_x)$	(2.1)
Mitochondrial Ca^{2+}	$\frac{dCa_m}{dt} = f_m(J_{MCU} - J_{NCX} + J_x)$	(2.2)
Inactivated IP_3R	$\frac{dR_i}{dt} = k_+ Ca_c^{n_i} \frac{1-R_i}{1+(\frac{Ca_c}{K_a})^{n_a}} - k_- R_i$	(2.3)
Mitochondrial NADH	$\frac{dNADH}{dt} = J_{PDH} - J_O + J_{AGC}$	(2.4)
Mitochondrial ADP	$\frac{dADP_m}{dt} = J_{ANT} - J_{F_1F_o}$	(2.5)
Cytosolic ADP	$\frac{dADP_c}{dt} = J_{HYD} - J_{ANT}$	(2.6)
MMP*	$\frac{dV_m}{dt} = (a_1 \cdot J_O - a_2 \cdot J_{F_1F_o} - J_{ANT} - J_{Hleak} - J_{NCX} - 2 \cdot J_{MCU} - 2 \cdot J_x - J_{AGC})/C_p$	(2.7)
Conservation equations		
Ca^{2+}	$\frac{Ca_c}{f_c} + \frac{\alpha Ca_r}{f_r} + \frac{\delta Ca_m}{f_m} = C_T$	(2.8)
NAD†	$NADH + NAD^+ = NAD_T$	(2.9)
Cytosolic AN‡	$ADP_c + ATP_c = AN_{cT}$	(2.10)
Mitochondrial AN‡	$ADP_m + ATP_m = AN_{mT}$	(2.11)

*Mitochondrial Membrane Potential, †Nicotinamide-Adenine Nucleotide, ‡Adenine Nucleotide.

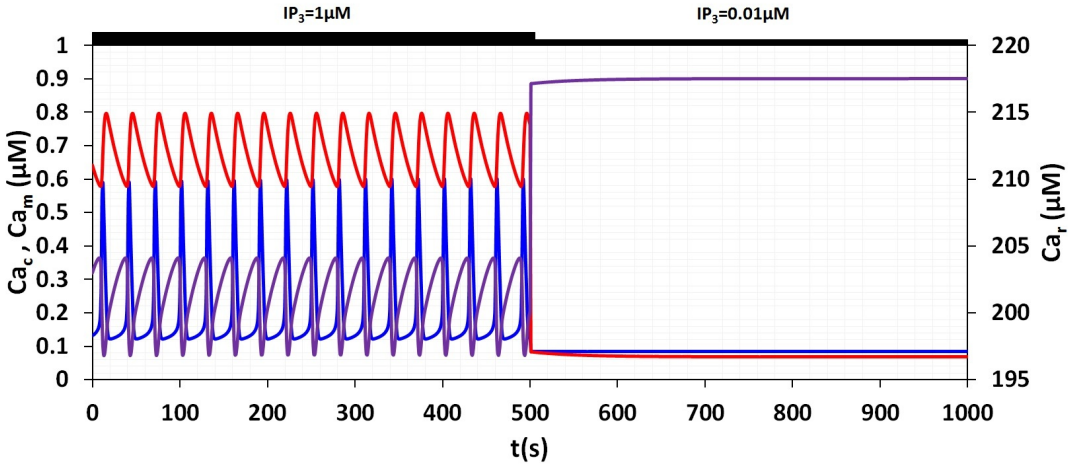

FIGURE 2.2: Temporal evolution of Ca^{2+} in cytosol (blue), mitochondria (red) and endoplasmic reticulum (purple), under a stimulated (IP_3= $1\mu M$) and a non-stimulated situation (IP_3= $0.01\mu M$).

The oscillatory behaviour shown in Figure 2.2 (for time below $500s$), is mainly due to the biphasic regulation of the IP_3 receptors at low and high cytosolic Ca^{2+} under stimulation. A deep analysis of the oscillations lets notice that a release of Ca_m leads to the increase in Ca_c and the replenishment of endoplasmic reticulum. The rise in Ca_c stimulates the IP_3R provoking a great release of Ca^{2+} from endoplasmic reticulum while Ca_m increases. Then, in agreement with experimental data (Ishii, Hirose, and Iino, 2006), it is possible to prove that mitochondria play a key role in shaping the whole Ca^{2+} dynamics via modelling and simulation (Wacquier et al., 2016; Wacquier et al., 2017). On the other hand, in the absence of stimulus (time above $500s$), the system reaches a non-oscillatory steady state, and the values of Ca^{2+} in each compartment are in accordance with quiescent conditions from different cell types (Babcock et al., 1997; Boyman et al., 2014; De Marchi et al., 2014).

It is worth noticing that WM is very stiff (see Appendix B), thus the numerical method used to integrate it was backward differentiation formula (BDF) of variable-step, and the maximum step size was defined as 0.1s, which represents the maximum size of a single step used.

2.3 A compartmental model lacking mitochondria

To take into account the crucial spatial aspects of cardiac cells, it was proposed to use the compartmental model of Grandi, Pasqualini, and Bers, 2010. That work was originally proposed as a tool to investigate the excitation-contraction coupling (ECC) and the repolarization phenomenon in a single *myocyte*. This model was based on the previously one developed by Shannon et al., 2004 for rabbit ventricular *myocytes*, but Grandi's model (GM) accounts for recent experimental data from human ventricular *myocytes*. Among

other important phenomena, GM is able to reproduce the human ventricular action potential and the Ca^{2+} transients in cytosol, subsarcolemmal space[3] and dyadic cleft (also called junctional cleft). Thus, this model provides a proper approximation of the different levels of Ca^{2+} within the cell, so it is suitable for investigating the hypothesis of this project.

The cellular structure considered by GM consists of four compartments (Figure 2.3), junctional cleft (j, dark green), subsarcolemmal space (s, light green), sarcoplasmic reticulum (r, purple) and bulk cytosol (c, light blue). The volume corresponding to each compartment is 0.0539%, 2%, 3.5% and 65% of the cell volume (33pL), respectively. The differential equations in GM include the change in membrane potential, the gating variables of the ion channels, and the intracellular ion concentrations; in total they are 38. In Table 2.2, the Na^+ and Ca^{2+} differential equations in each compartment are pointed out, while the full expression of the fluxes and the model parameters are in Grandi, Pasqualini, and Bers, 2010.

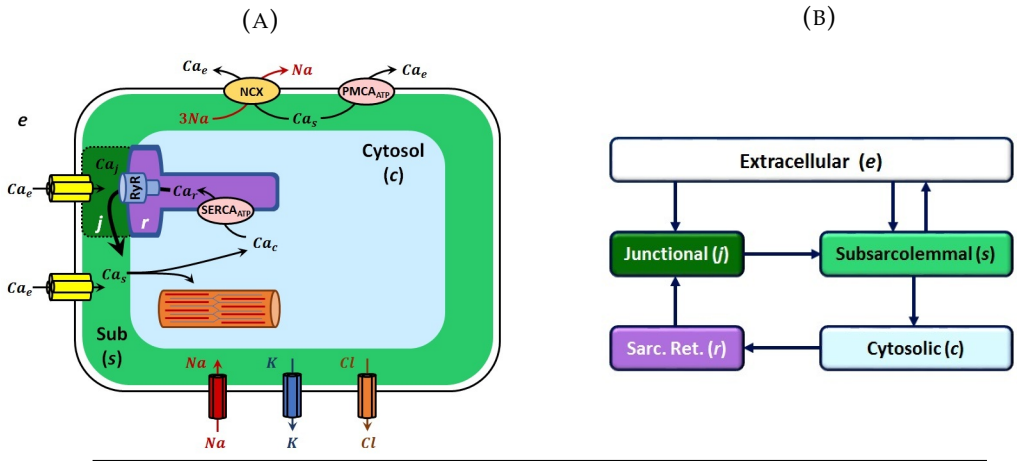

FIGURE 2.3: (A) Schematic representation of the four compartments in the cellular structure considered by the model of Grandi, Pasqualini, and Bers, 2010. (B) Direction of Ca^{2+} fluxes among compartments.

In Figure 2.4, the pattern of each ion current during the action potential is shown, and the differential equation describing the membrane potential (shown in the bottom right panel) is $\dot{V} = (I_{tot} - I_{app})$; where I_{app} is the current applied, that is, the depolarization coming from the sinoatrial nodule, and I_{tot} is the sum of all ion currents. It is worth noticing that this latter current shapes the cardiac action potential (see Figure 2.5 and Figure 2.4). Finally, to highlight the behaviour of Ca^{2+} in each compartment of GM, in Figure 2.6 is shown the simulation of these concentrations as in Grandi, Pasqualini, and Bers, 2010.

[3]Subsarcolemmal space is the region just under the sarcolemmal membrane that is not in front of the RyR channels (sarcoplasmic reticulum), thus it is not part of the dyadic cleft.

TABLE 2.2: Ion homeostasis of Grandi's Model.

Compartment	Na^+ and Ca^{2+} differential equation	Number
Junctional cleft (j)	$\frac{dNa_j}{dt} = -\frac{I_{NaTj}C_m}{V_jF} + \frac{J_{Najs}}{V_j}(Na_s - Na_j) - \frac{dNa_{Bj}}{dt}$	(2.12)
	$\frac{dCa_j}{dt} = -\frac{I_{CaTj}C_m}{2V_jF} + \frac{J_{Cajs}}{V_j}(Ca_s - Ca_j) - J_{CaBj} + \frac{J_{rCarel}V_r}{V_j} + \frac{J_{rleak}V_c}{V_j}$	(2.13)
Subsarcolemmal space (s)	$\frac{dNa_s}{dt} = -\frac{I_{NaTs}C_m}{V_sF} + \frac{J_{Najs}}{V_s}(Na_j - Na_s) + \frac{J_{Nasc}}{V_s}(Na_c - Na_s) - \frac{dNa_{Bs}}{dt}$	(2.14)
	$\frac{dCa_s}{dt} = -\frac{I_{CaTs}C_m}{2V_sF} + \frac{J_{Cajs}}{V_s}(Ca_j - Ca_s) + \frac{J_{Casc}}{V_s}(Ca_c - Ca_s) - J_{CaBs}$	(2.15)
Bulk cytosol (c)	$\frac{dNa_c}{dt} = \frac{J_{Nasc}}{V_c}(Na_s - Na_c)$	(2.16)
	$\frac{dCa_c}{dt} = -\frac{J_{SerCa}V_r}{V_c} - J_{CaBc} + \frac{J_{Casc}}{V_c}(Ca_s - Ca_c)$	(2.17)
Sarcoplasmic reticulum (r)	$\frac{dCa_r}{dt} = J_{SerCa} - \frac{J_{rleak}V_c}{V_r} - J_{Carel} - \frac{dCa_{sqnb}}{dt}$	(2.18)

It is worth noticing that as in WM, the numerical method used to integrate GM was backward differentiation formula (BDF) of variable-step, also due to the stiffness of the system of differential equations (see Appendix B), but in this case, the maximum step size was defined as 0.1ms.

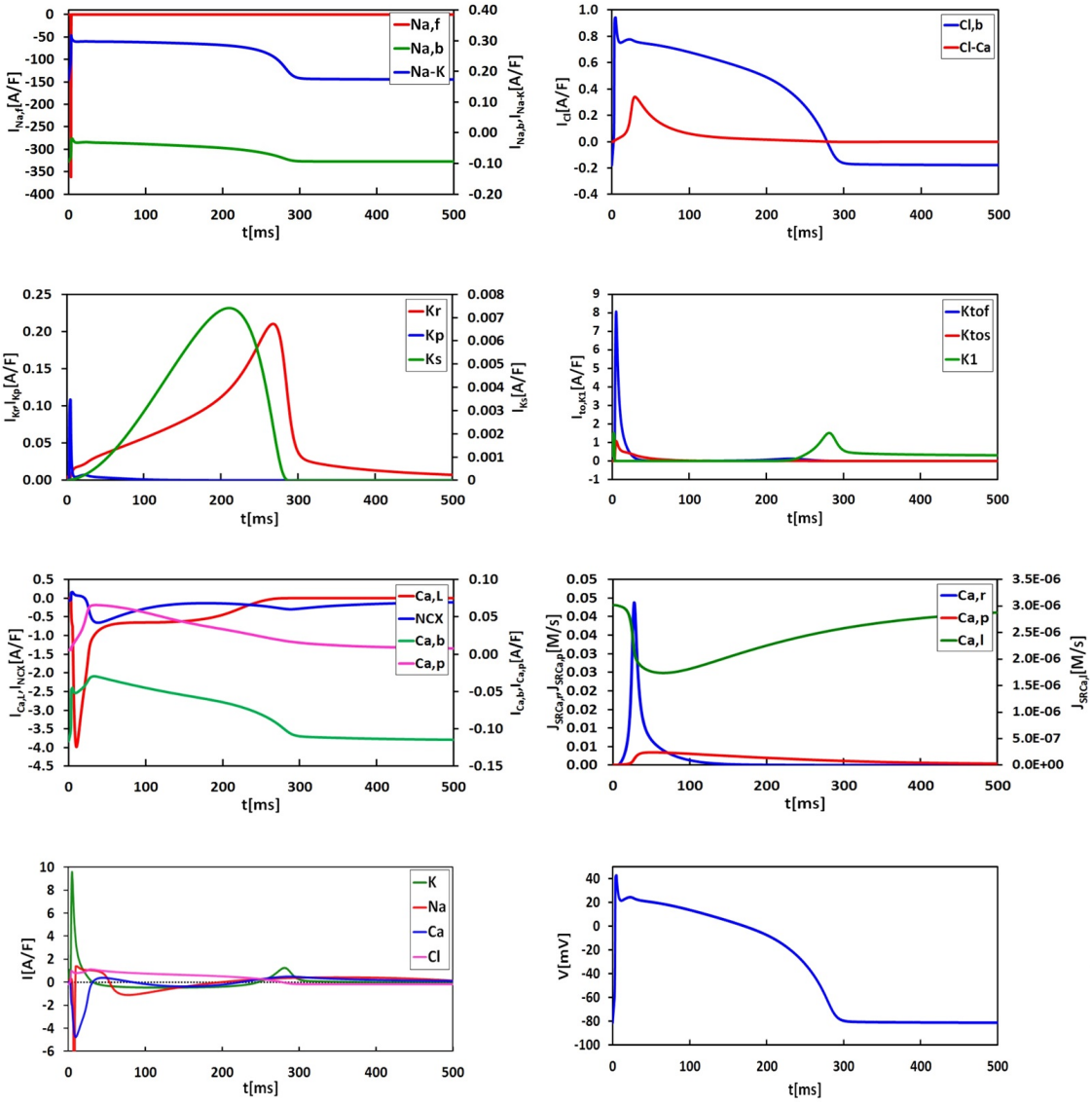

FIGURE 2.4: Contribution of each ion current to the action potential shape (bottom right).

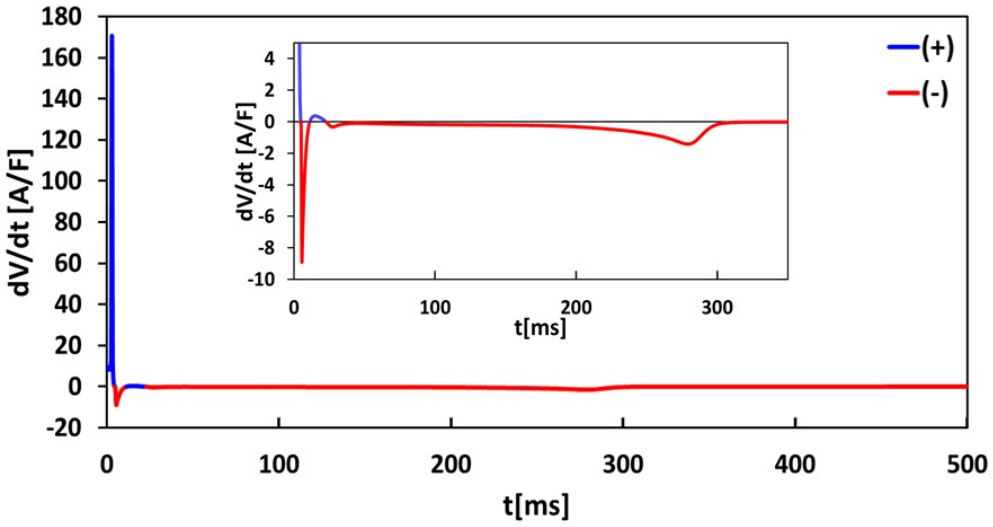

FIGURE 2.5: Derivative of the membrane potential calculated through its differential equation over the range of the cardiac action potential. Inset: zoom between 0 and 350ms with plot range equal to [-10,5]. See also 2.4 for comparison with the membrane potential behaviour.

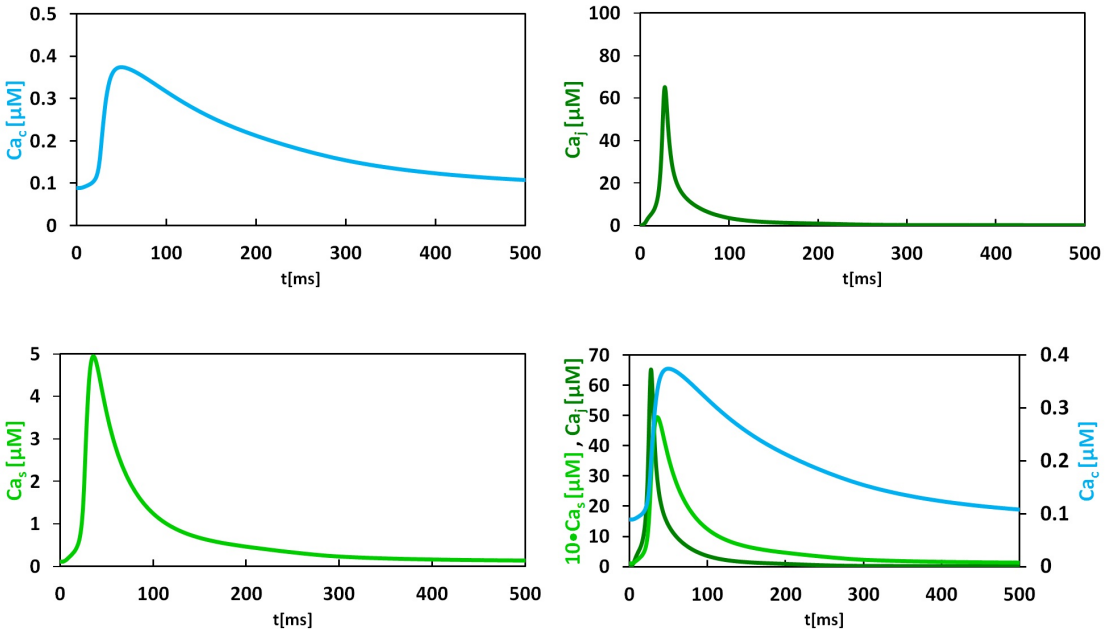

FIGURE 2.6: Kinetics of cytosolic (c), junctional (j) and subsarcolemmal (s) Ca^{2+} during the cardiac action potential; simulations using the model of Grandi, Pasqualini, and Bers, 2010.

Chapter 3

Project approach

3.1 Hypothesis

The spatial location of mitochondria plays a crucial role in Ca^{2+} dynamics and mitochondrial metabolism in cardiac cells.

3.2 Justification

Regulation mechanisms of intracellular Ca^{2+} in cardiac *myocytes* generate a highly organized spatial and temporal dynamics on which underlies excitation-contraction coupling and regulation of mitochondrial energy metabolism. All these are vital processes for the proper functioning of the heart.

Interplay between Ca^{2+} dynamics and mitochondrial metabolism in cardiac *myocytes* has been studied for several years through experimental methods. However, results are still controversial. Thus, an alternative to elucidate the underlying mechanisms of this phenomenon is a modelling and simulation approach.

In addition, studying of the reaction-diffusion process on a cardiac *myocyte* region including mitochondria and dyadic cleft is challenging even through computational implementation. This is because of the regulation mechanisms of Ca^{2+}, which lead to stiff mathematical models whose complexity increases notably when the inherent heterogeneity of the system is considered.

Finally, some cardiac pathologies are clearly related to alterations in ATP production. However, dynamic measurements of the production of ATP by mitochondria are technically difficult to realize. Thus, modelling can provide a useful tool to support experimental investigations on the origins of these pathologies.

Based on the above, the development of a computational model to study Ca^{2+} dynamics on a two-dimensional region of cardiac *myocyte* is really interesting. The aim of our modelling approach is to evaluate the changes in Ca^{2+} dynamics and mitochondrial metabolism when mitochondria is located at different distances from the dyadic cleft.

3.3 Aims

3.3.1 General aim

To develop a model of the spatial Ca^{2+} dynamics that allows the study of its participation on the mitochondrial metabolism in cardiac cells.

3.3.2 Specific aims

[1] To propose a model of Ca^{2+} dynamics in cardiac cells.

[2] To solve numerically the proposed model through comparmental modelling approach.

[3] To evaluate if mitochondrial position modifies Ca^{2+} dynamics and mitochondrial metabolism.

3.4 Project steps

In Figure 2.5, the block diagram of the procedure to reach the aims is shown. In the first two steps an adequate spatiotemporal model of Ca^{2+} dynamics in cardiac cells will be developed, while in the latest, the computational study of the interplay between Ca^{2+} dynamics and mitochondrial metabolism will be performed.

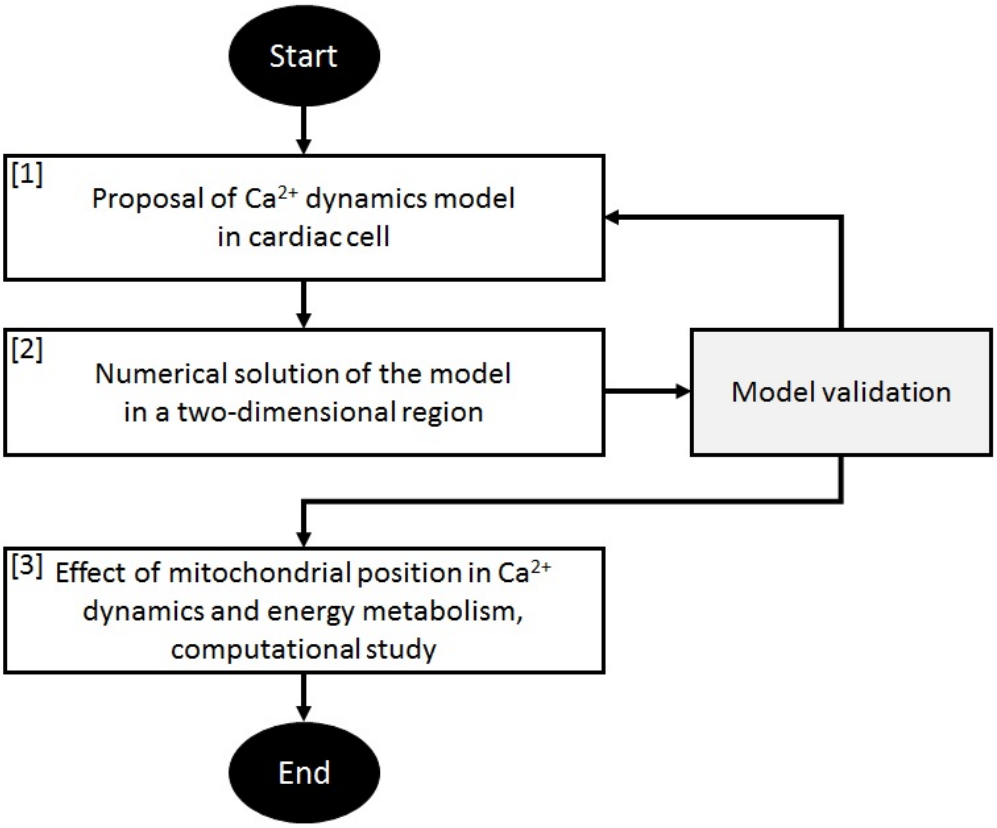

FIGURE 3.1: Project steps.

Chapter 4

Results

4.1 The mitochondrial model

4.1.1 Modelling Ca^{2+} signalling

To obtain the results about Ca^{2+} signalling, WM was implemented as reported in Chapter 2. Once it was completed, it was necessary to take into account the particular features of mitochondria in *cardiomyocytes*. In Table 4.1 the principal mechanisms of mitochondrial Ca^{2+} influx and efflux in this cell type are presented and briefly described. It is important to notice that there are some other mechanisms proposed to play a role in mitochondrial Ca^{2+} regulation, but most of the them are not well established; more details could be find in Dedkova and Blatter, 2013.

WM accounts for MCU and mNCX, and it also has a leak current proposed to play a low conductance mPTP-like mechanism, which is a channel of the inner mitochondrial membrane operating in two distinct physiological pathways: the Ca^{2+} signalling during life (at its low conductance state), and the Ca^{2+}-dependent cell death (at its high conductance state) (Bernardi and Di Lisa, 2015; Ichas and Mazat, 1998). Finally, the two remaining mechanisms, that is, RaM and mRyR1, are not considered in this project because the first one is unlikely to be active at normal Ca^{2+} levels into cell and the second one is still matter of discussion.

The usage of WM was intended to reproduce the experimental results of Sedova, Dedkova, and Blatter, 2006. In that work, the authors used a pressure-ejection system through which they were able to impose cytosolic Ca^{2+} transients in permeabilized ventricular *myocytes*, finally they followed the dynamic of mitochondrial Ca^{2+}. Equations 2.2, 2.4 and 2.7 (see Table 2.1) of WM were used for modelling mitochondrial Ca^{2+} homeostasis of *cardiomyocytes*, and its necessary modifications are described below.

- The first modification was the particular volume of each organelle in *cardiomyocytes*. It is taken into account through the volume ratio between mitochondria and cytosol. In this sense, an interesting characteristic of *cardiomyocytes* is its larger mitochondrial volume in comparison with other cell types Fieni et al., 2012. In Table 4.2, the parameters of Ca^{2+} fluxes involved in this modification are expressed in terms of cytosolic volume aiming to be properly scaled using the real volume of each compartment from *cardiomyocytes* in further applications.

TABLE 4.1: Main mechanisms of mitochondrial Ca^{2+} influx and efflux.

Mechanism	Observations	Reference
MCU	This mechanism of Ca^{2+} uptake called Mitochondrial Calcium Uniporter uses the electrochemical gradient of mitochondrial membrane as motive force, and has several positive and negative modulators (e.g. adenine nucleotides). In addition, this is the most studied influx manner and extensively accepted as the main mechanism controlling the influx of Ca^{2+} into mitochondria.	Baughman et al., 2011; Dedkova and Blatter, 2008
RaM	The rapid mode of Ca^{2+} uptake is several times faster than MCU, but is inactive at extra-mitochondrial Ca^{2+} concentrations above 100nM. That plus the fact that RaM requires between 60 and 90 seconds for total recovery, suggest that RaM does not play a key role for mitochondrial Ca^{2+} homeostasis in *cardiomyocytes* under normal conditions.	Bazil and Dash, 2011; Buntinas et al., 2001
mRyR1	This influx mechanism has been proposed to be crucial as a fast mode of Ca^{2+} uptake within physiological Ca^{2+} concentrations (μM) with a bell shaped dependence on cytosolic Ca^{2+} and it is characterized by having similar properties as the ryanodine receptor type 1 (RyR1) found in the ER membrane of skeletal muscles.	Beutner et al., 2005; Ryu et al., 2010
mNCX	Although several Na^{+}-dependent and -independent mechanisms of Ca^{2+} efflux have been proposed, it is well established that the also called mNCLX is the main extruder of Ca^{2+} from mitochondria. This is an electrogenic Na^{+}-Ca^{2+} exchanger depending on the concentration of both ions and on the MMP.	Beutner et al., 2005; Ryu et al., 2010

- The second modification comes from the fact that the system cannot longer be considered closed due to the cell permeabilization presented in Sedova, Dedkova, and Blatter, 2006. Then, Equation 4.1 (Table 4.3) reproduces the square-wave Ca^{2+} pulses imposed by the pressure-ejection system described above. In this function, Ca_{ba} is the basal cytosolic Ca^{2+} level, Ca_{max} represents de amplitude of the pulse, H is the heaviside function, t_{on} is the duration of the Ca^{2+} pulse and *mod* is the modulo function whose variables are time and the period of the square-wave (τ).

TABLE 4.2: Parameters of Ca^{2+} fluxes in terms of cytosolic volume.

Flux	Original units	Parameter[a]	Original value (WM)	Respect to cytosolic volume[b]
J_{MCU}	$\frac{\mu molCa^{2+}}{L_m \cdot s}$	V_{MCU}	$0.0006 \frac{\mu molCa^{2+}}{L_m \cdot s}$	$0.0006\delta = 4.4 \cdot 10^{-5} \frac{\mu molCa^{2+}}{L_c \cdot s}$
J_{NCX}	$\frac{\mu molCa^{2+}}{L_m \cdot s}$	V_{NCX}	$0.35 \frac{\mu molCa^{2+}}{L_m \cdot s}$	$0.35\delta = 0.0257 \frac{\mu molCa^{2+}}{L_c \cdot s}$
J_x	$\frac{\mu molCa^{2+}}{L_m \cdot s}$	$k_x \cdot \Delta C$	$0.008 \frac{1}{s}$	$0.008\delta = 5.9 \cdot 10^{-4} \frac{1}{s}$

(a) Although k_x have units of $\frac{1}{s}$, it is defined with respect to mitochondrial volume, as they are multiplied by the Ca^{2+} concentration gradients.

(b) $\delta = 0.0733$ is the ratio of the cell compartment volumes in WM.

For Equations 4.2-4.4, the volumes are those from the cell compartments in a ventricular *myocyte* (Grandi, Pasqualini, and Bers, 2010), and the fluxes parameters are in agreement to flux balance in Table 4.2. However, it is important to notice that J_{MCU} and J_{NCX} had to be further modified.

TABLE 4.3: Equations for describing cardiac mitochondria.

Variable	Equation	Number
Cyt. Ca^{2+}	$Ca_c = Ca_{ba} + (Ca_{max} - Ca_{ba})H(t_{on} - mod(t, \tau))$	(4.1)
Mit. Ca^{2+}	$\frac{dCa_m}{dt} = f_m(J_{MCU} - J_{NCX} + J_x)V_c/V_m$	(4.2)
Mit. NADH	$\frac{dNADH}{dt} = (J_{PDH} - J_O + J_{AGC})V_c/V_m$	(4.3)
MMP	$\frac{dV_m}{dt} = \frac{1}{C_p}(a_1 \cdot J_O - J_{Hleak}V_m/V_c - J_{NCX} - 2 \cdot J_{MCU} - 2 \cdot J_x - J_{AGC})V_c/V_m$	(4.4)

- The third modification is related to the magnitude of the MCU flux, which has been reported to be much smaller in *myocytes* than in other cell types (Fieni et al., 2012; Williams et al., 2013). In order to keep the original expression of WM for MCU flux, it was contrasted versus the equation proposed by Williams et al., 2013, which fits to several experimental data (see Table C.1). It was found that MCU flux expression of WM can account for the behaviour described by Equation B.1 when modifying the affinity of MCU to Ca^{2+} (parameters K_1 and K_2) and by decreasing the density of MCU expression in cardiac cells through V_{MCU} parameter (see Figure C.1); these changes are in agreement with the findings of Paillard et al., 2017. In addition, the MCU flux expression of WM has been successfully used to model *myocytes* MCU flux (Wacquier et al., 2017).

- The last modification was the usage of the original J_{NCX} expression from Cortassa et al., 2003 because of both the presence of Na^+ as an explicit variable in the following simulations and the inaccurate of the J_{NCX} expression from Wacquier et al., 2016 in broad ranges of Ca_m.

4.1.2 Validation

In Table 4.4 are the values for each parameter of the mitochondrial model (MM) for reproducing the experimental results of Sedova, Dedkova, and Blatter, 2006.

TABLE 4.4: Meaning and value of mitochondrial model parameters.

Parameter	Definition	Value	Reference
a_1	Scaling factor between NADH consumption and change in membrane voltage	20	Wacquier et al., 2016
b_{NCX}	V_m dependence of NCX	0.5	Cortassa et al., 2003
C_p	Mitochondrial inner membrane capacitance divided by F	$1.8\frac{\mu M}{mV}$	Bertram et al., 2006
δ	Volumic ratio between the mito, and the cytosol in WM	0.0733	Bertram et al., 2006
F	Faraday constant	$96480\frac{C}{mol}$	NA
f_m	Fraction of free over buffer-bound Ca^{2+} in mitochondria	0.00017	This work
K_1	Dissociation constant for Ca^{2+} translocation by the MCU	$21\mu M$	This work
K_2	Dissociation constant for MCU activation by Ca^{2+}	$1.33\mu M$	This work
K_{AGC}	Dissociation constant of Ca^{2+} from AGC	$0.14\mu M$	Contreras et al., 2007
k_{GLY}	Velocity of glycolysis (empirical)	$450\frac{\mu M}{s}$	Bertram et al., 2006
k_o	Rate constant of NADH oxidation by ETC	$600\frac{\mu M}{s}$	Bertram et al., 2006
k_x	Rate constant of bidirectional Ca^{2+} leak from mitochondria	$5.9 \cdot 10^{-4}/s$	Wacquier et al., 2016
K_{Na}	Affinity constant of NCX to Na^+	$9.4mM$	Cortassa et al., 2003
K_{Ca}	Affinity constant of NCX to Ca^{2+}	$0.375\mu M$	Cortassa et al., 2003
L	Allosteric equilibrium constant for uniporter conformations	50	Magnus and Keizer, 1998
NAD_T	Total concentration of mitochondrial pyridine nucleotides	$250\mu M$	Wacquier et al., 2016
p_1	Voltage dependence coefficient of MCU activity	$0.1/mV$	Wacquier et al., 2016
p_2	Voltage dependence coefficient of NCX activity	$0.016/mV$	Wacquier et al., 2016
p_3	Voltage dependence coefficient of calcium leak	$0.05/mV$	Wacquier et al., 2016
p_4	Voltage dependence coefficient of AGC activity	$0.01/mV$	Wacquier et al., 2016
q_1	Michaelis-Menten-like constant for NAD^+ consumption by the Krebs cycle	1	Bertram et al., 2006
q_2	$S_{0.5}$ value for activation the Krebs cycle by Ca^{2+}	$0.1\mu M$	Wacquier et al., 2016
q_x	$S_{0.5}$ value for value for indirect inhibition of the AGC by cytosolic Ca^{2+}	$0.1\mu M$	Wacquier et al., 2016

Continue

Table 4.4: Meaning and value of mitochondrial model parameters.

Parameter	Definition	Value	Reference
q_3	Michaelis-Menten constant for NADH consumption by the ETC	$100\mu M$	Bertram et al., 2006
q_4	Voltage dependence coefficient 1 of ETC activity	$177mV$	Bertram et al., 2006
q_5	Voltage dependence coefficient 2 of ETC activity	$5mV$	Bertram et al., 2006
q_9	Voltage dependence of the proton leak	$2\frac{\mu M}{s \cdot mV}$	Bertram et al., 2006
q_{10}	Rate constant of the voltage-independent proton leak	$-30\frac{\mu M}{s}$	Bertram et al., 2006
R	Perfect gas constant	$8315\frac{mJ}{mol \cdot K}$	NA
T	Temperature	$310.16K$	NA
V_{AGC}	Rate constant of NADH production via malate-aspartate shuttle	$25\frac{\mu M}{s}$	Wacquier et al., 2016
V_{MCU}	Rate constant of the MCU	$1.5 \cdot 10^{-5}\frac{\mu M}{s}$	This work
V_{NCX}	Rate constant of the NCX	$4.4\frac{\mu M}{s}$	Bertram et al., 2006

In a first step, a code for simulating the experiment of imposed cytosolic Ca^{2+} transients through the pressure-ejection system described in the previous section was made. As shown in Figure 4.1, mitochondria slowly integrate Ca_c spiking, which is in agreement with the findings of Sedova, Dedkova, and Blatter, 2006 and others (see Dedkova and Blatter, 2013).

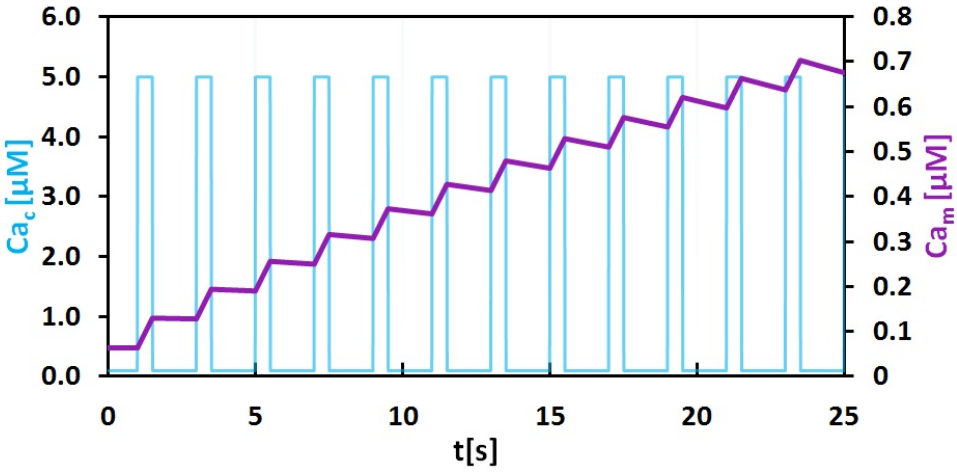

FIGURE 4.1: Slowly integration of Ca_c spiking by mitochondria. $\tau = 2s$, $t_{on} = 0.5s$, $Na_c = 20mM$. Reproduction of Figure 6C from Sedova, Dedkova, and Blatter, 2006.

In a next step, the dependence of Ca_m on the duration and frequency of Ca_c transients (Sedova, Dedkova, and Blatter, 2006) was validated (Figure 4.2). As in experimental results, the kinetic of mitochondrial calcium uptake is strongly related to both duration and frequency of the imposed cytosolic calcium spikes. As duration time increases, integrated mitochondrial calcium increases too, while the dependence on frequency is analogue (notice that in Figure 4.2B, the label of the series indicates the period, that is, the inverse of frequency). Even, the minor integration of Ca^{2+} at $t_{on} = 0.2s$ and $f = 0.25Hz \rightarrow \tau = 4s$, or $f = 0.25Hz \rightarrow \tau = 4s$ and $t_{on} = 0.5s$ (Sedova, Dedkova, and Blatter, 2006), was properly simulated (Figure 4.2).

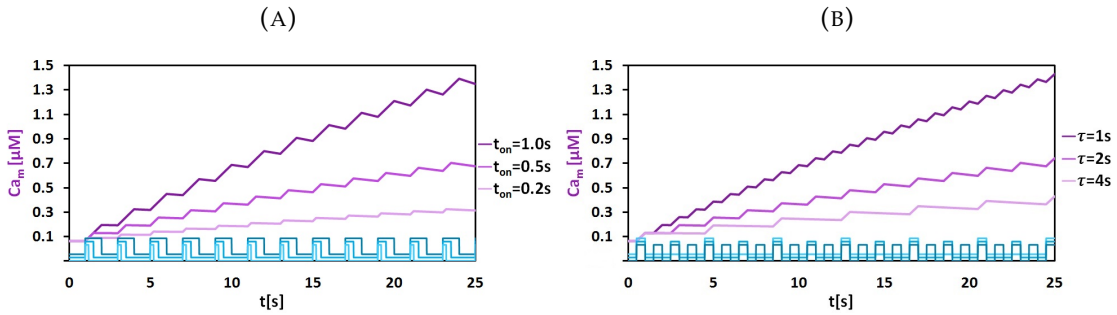

FIGURE 4.2: Effect of duration and frequency of Ca_c transients on mitochondrial calcium uptake. (A) Effect of changing the duration t_{on} of Ca_c transients at constant frequency, $f = 0.5Hz \rightarrow \tau = 2s$. (B) Effect of changing the frequency (or period τ) of Ca_c transients at constant duration, $t_{on} = 0.5s$. In all cases, $Na_c = 20mM$. Reproduction of Figure 7 from Sedova, Dedkova, and Blatter, 2006.

4.2 Coupled model (compartmental + mitochondrial)

After validation of MM for describing *cardiomyocytes* mitochondria, this model was inserted in GM aiming to get a more comprehensive model that permits investigate the working hypothesis, that is, to proof that the exact location of mitochondria plays a crucial role in determining of Ca^{2+} dynamics and mitochondrial metabolism for cardiac cells. Three scenarios (S1, S2 and S3) of how Ca^{2+} signalling is affected depending on mitochondrial position were proposed (see Figure 4.4). The simplest scenario is when mitochondria only interacts with cytosol, and it was used to validate the coupled model. The comparison between compartmental model and coupled model (S1) is shown in Figure 4.3.

It was a very interesting finding that when inserting MM in GM, Ca^{2+} dynamics in each compartment (cytosol, junctional and subsarcolemmal) is almost exactly the same as in Grandi, Pasqualini, and Bers, 2010; indeed, the maximum value in all cases differentiates in less than 0.4%. In addition, the maximum of value of the membrane potential differentiates in less than 0.01%.

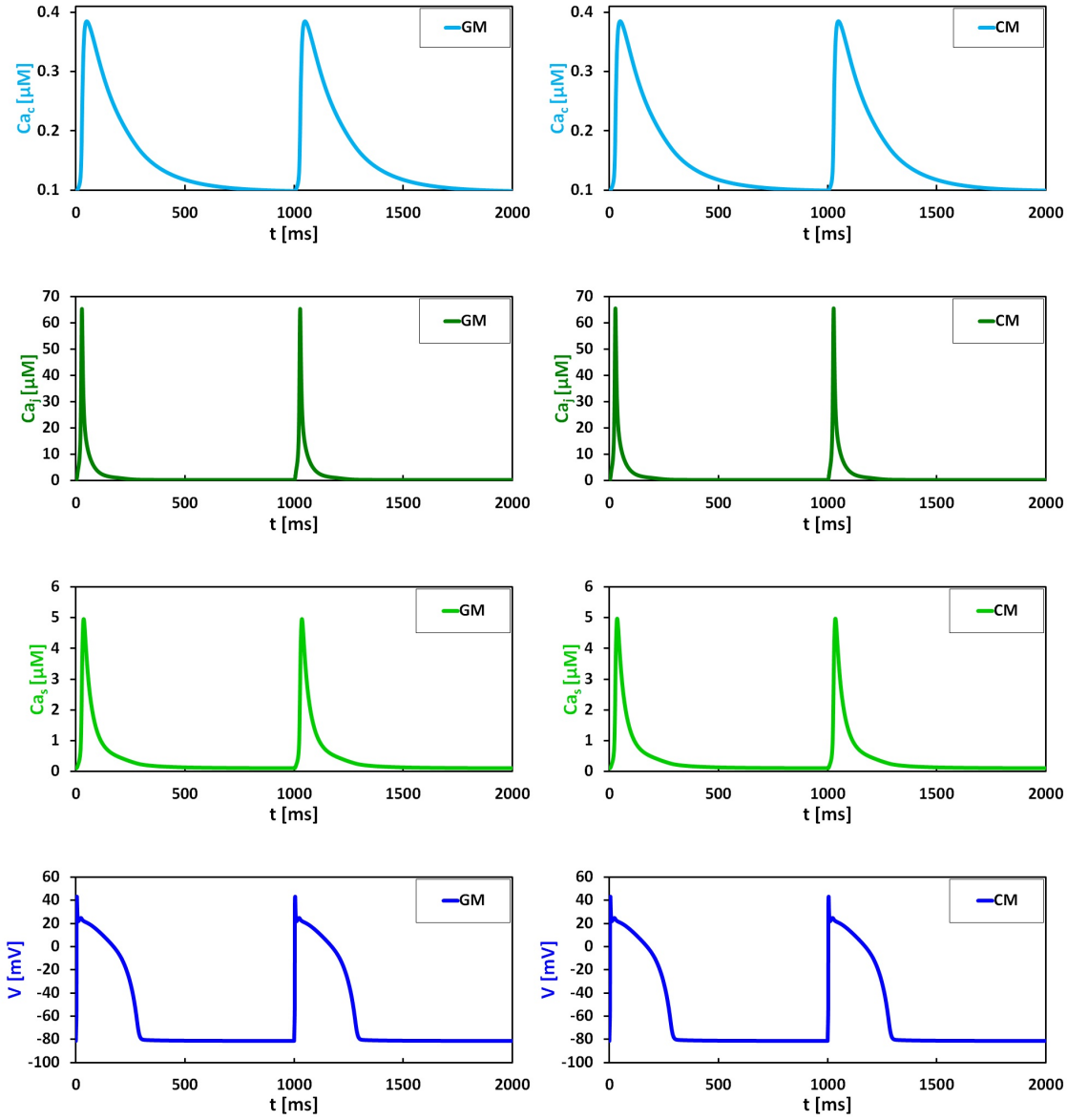

FIGURE 4.3: Validation of the Coupled Model. Simulation of Ca^{2+} dynamics and cardiac action potential using GM (left panels) and using CM (right panels).

4.3 Effect of mitochondrial position on Ca^{2+} dynamics

The three scenarios proposed to analyse the effect of mitochondrial position on Ca^{2+} dynamics correspond to the compartmental arrangements shown in Figure 4.4 (left panels). First of all, it is important to notice that since junctional space is very narrow, mitochondria have no possibility of uptake Ca^{2+} from this compartment. Thus, the region of highest Ca^{2+} concentration interacting with mitochondria is the subsarcolemmal space, while cytosolic Ca^{2+} also can enters into mitochondria via MCU.

Based on the above, the scenarios to study the effect of mitochondrial position are:

S1: Mitochondria only interacts with cytosol.

S2: Mitochondria interacts with both cytosol and subsarcolemmal space.

S3: Mitochondria only interacts with subsarcolemmal space.

To model S1, just the addition of the MM fluxes (J_{MCU} and J_{NCX}) into the differential equation of cytosolic Ca^{2+} was necessary, while all the other equations remained unchanged. In the case of S3, the same fluxes were added to the subsarcolemmal Ca^{2+} differential equation. However, it is important to keep in mind that sodium and calcium are variables in each compartment of the CM, thus the expression for each flux depends on the corresponding concentrations. For example, J_{NCX} in S3 depends on Ca_s, Ca_m, and Na_s.

To model S2, expressions for J_{MCU} and J_{NCX} were introduced taking into account a specific fraction of interaction with cytosol and subsarcolemmal space. For Equations in Table 4.5, "r" and "$1-r$" are the fractions of mitochondrial fluxes interacting with cytosol and subsarcolemmal space, respectively. In Equations 4.5 and 4.6, the variables in the square brackets are those on which depend J_{MCU} and J_{NCX}. While in Equations 4.7 and 4.8, the fluxes with "GM" subscript represents all the original fluxes in the cytosolic and subsarcolemmal Ca^{2+} differential equations in the model of Grandi, Pasqualini, and Bers, 2010 (see Equations 2.17 and 2.15).

TABLE 4.5: Fluxes and dynamics equations for modelling S2.

Flux/Var.	Equation	Number
J_{MCU}	$J_{MCU} = r \cdot J_{MCU}[Ca_c] + (1-r)J_{MCU}[Ca_s]$	(4.5)
J_{NCX}	$J_{NCX} = r \cdot J_{MCU}[Ca_c, Ca_m, Na_c] + (1-r)J_{MCU}[Ca_s, Ca_m, Na_s]$	(4.6)
Cyt. Ca^{2+}	$\frac{dCa_c}{dt} = J_{Ca_{c,GM}} + r(-J_{MCU} + J_{NCX} - J_x)$	(4.7)
Sub. Ca^{2+}	$\frac{dCa_s}{dt} = J_{Ca_{s,GM}} + (1-r)(J_{MCU} - J_{NCX} + J_x)$	(4.8)

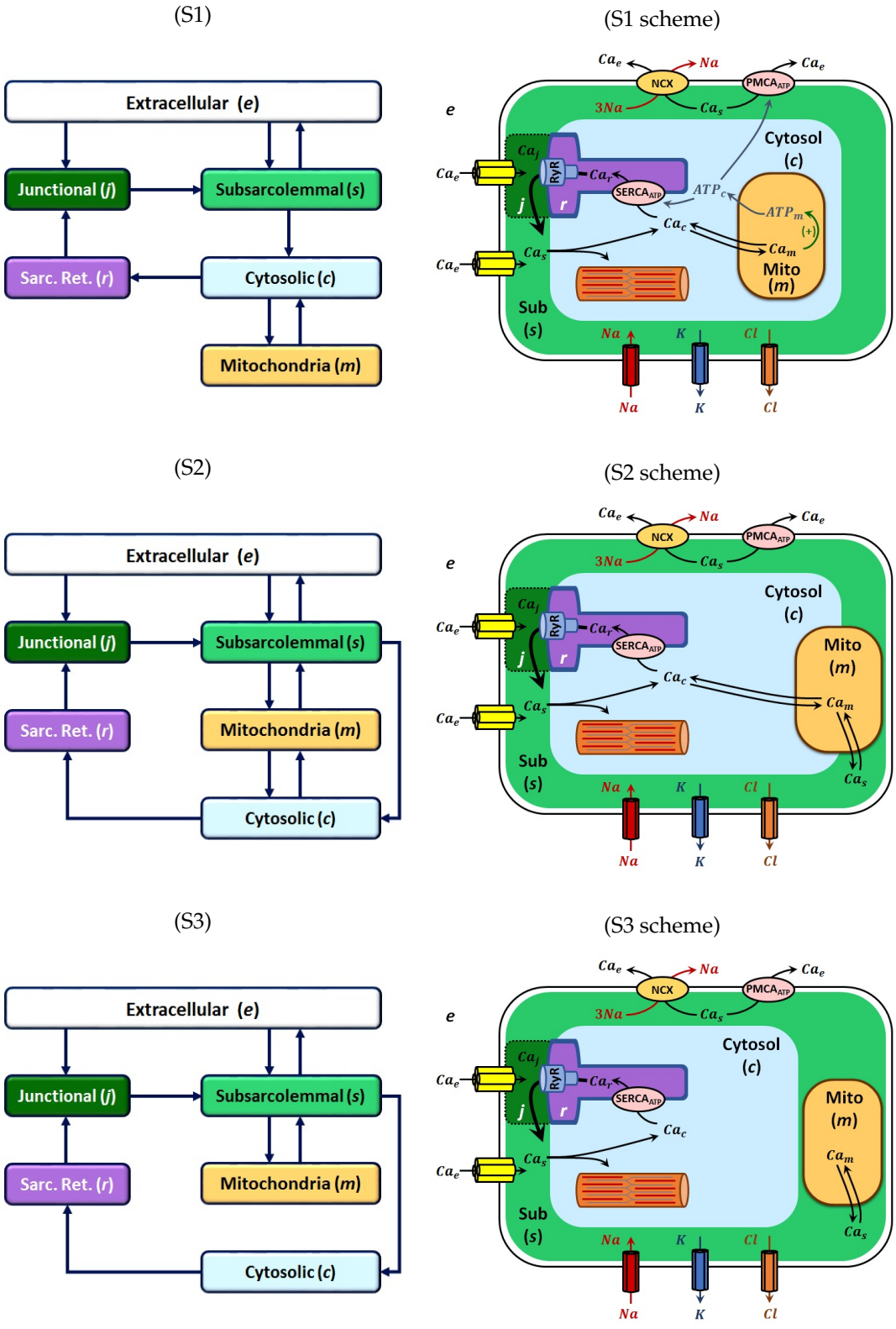

FIGURE 4.4: Compartmental configurations to study the effect of mitochondrial position in *cardiomyocytes*. Direction of Ca^{2+} fluxes among compartments in each scenario (left panels). Schematic representation of each scenario (right panels). Illustration of Ca^{2+} effect on ATP synthesis (S1 scheme).

In fact, S2 represents the general problem to analyse the effect of mitochondrial location on Ca^{2+} dynamics. S1 and S3 can be modelled with the equations of S2 when "$r = 1$" and "$r = 0$", respectively. It is important to mention that in the following analysis the fraction used for S2 is "$r = 0.5$".

Ca^{2+} dynamics simulation of each scenario (S1, S2 and S3) is shown in Figure 4.5. As can be seen, the location of mitochondria greatly modifies the reached values of Ca^{2+} concentration in each compartment while no modifying the oscillation shape. Highest differences are in cytosolic compartment. S2 and S3 produce a peak at about 85% and 97% of S1, respectively (Figure 4.5A). For junctional and subsarcolemmal calcium, the maximum values reached in S2 are about 1.2% and 0.7% above those reached in S1. While S3 values reached in the same compartments are about 4.5% and 4% below S1 values (Figures 4.5B and 4.5C). Interestingly, it was also observed that in spite of the changes in Ca^{2+} dynamics, there was almost no effect on the cardiac action potential (their maximum values differ in less than 0.1%).

The distribution of Ca^{2+} in each compartment for S1, S2 and S3 is mainly due to the different gradients stablished as a consequence of mitochondria presence and its different interaction with the cytosolic and subsarcolemmal compartments. It was verified by watching at the transition phase of each scenario, that is, the Ca^{2+} dynamics immediately after starting the simulation at same initial values (first seconds in Figure 4.6).

Of particular interest is the evolution of mitochondrial Ca^{2+}. The simulations presented in Figure 4.6 let realize that, in contrast with the other compartments, mitochondrial Ca^{2+} dynamics is greatly determined by the spatial location of mitochondria, not only in quantitative terms, but also in the shape of the oscillations (see the inset in Figure 4.6). The steady oscillatory regime reached in S1 for Ca_m is at around a hundred nanomolar, while in S2 and S3 it is in the order of hundreds and thousands of nanomolar, respectively. This fact is in agreement with the initial idea that mitochondrial position can explain, at least in part, the wide range of mitochondrial Ca^{2+} concentrations measured experimentally (Dedkova and Blatter, 2013; Palmer et al., 2006). Finally, based on the demonstrated interplay between mitochondrial Ca^{2+} and the energetic variables (Wacquier et al., 2016), the found differences in mitochondrial calcium dynamics are a preamble of the dependence of energetic metabolism on the mitochondrial position in *cardiomyocytes*.

(A)

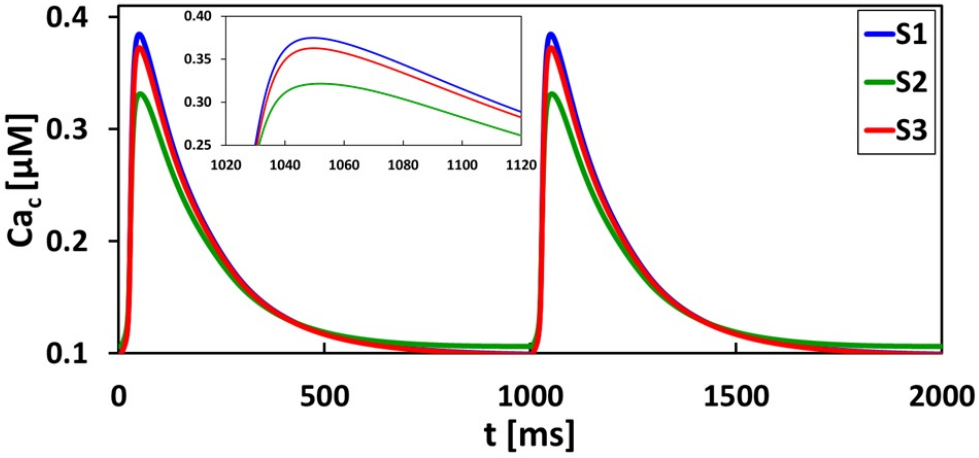

(B)

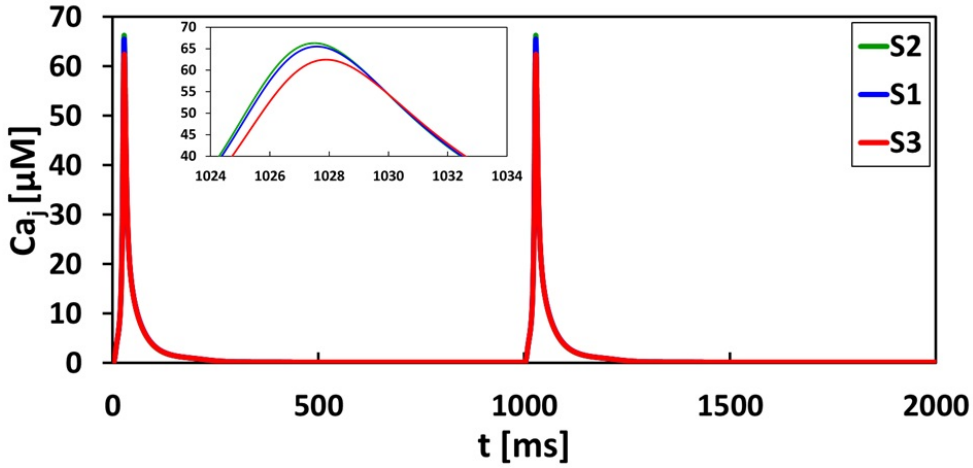

(C)

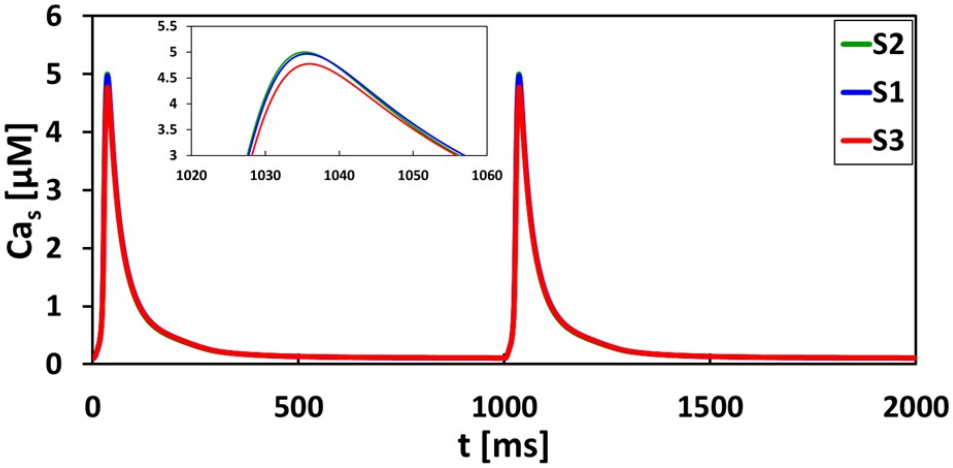

FIGURE 4.5: Effect of mitochondrial position on *cardiomyocytes* Ca^{2+} dynamics. Comparison of cytosolic (A), junctional (B) and subsarcolemmal (C) Ca^{2+} dynamics in each scenario (S1, S2 and S3).

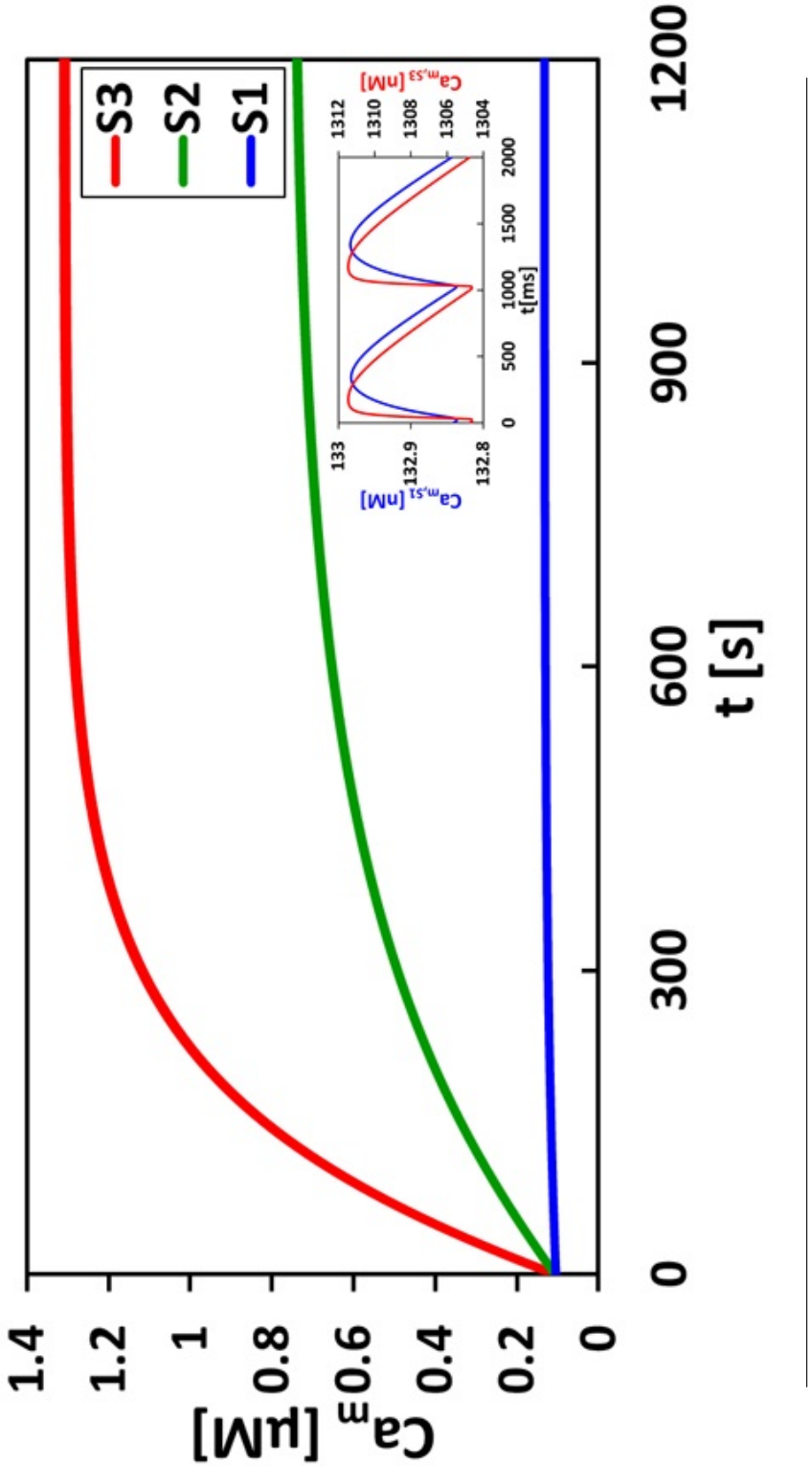

FIGURE 4.6: Effect of mitochondrial position on *cardiomyocytes* mitochondrial Ca^{2+} dynamics. Mitochondrial Ca^{2+} oscillations at the steady oscillatory regime, in the same time interval as in Figure 4.5 (inset).

Chapter 5

Conclusions

[1] Biological systems as *cardiomyocytes* are characterized by their complexity leading to highly stiff mathematical models. Then special numerical methods as backward differentiation formula are necessary to solve them.

[2] A very useful approach to simulate steep concentration gradients of microdomains is the called Common-Pool method, which is actually a compartmental modelling approach. In the biological system studied in this work, it allowed to get a realistic description of the dyadic cleft and the subsarcolemmal space, which are characterized by containing large amounts of Ca^{2+} in a very small space.

[3] The problem of simulating the spatial Ca^{2+} dynamics of *cardiomyocytes* can be addressed by compartmental modelling. Thereby, a compartmental model able to reproduce Ca^{2+} dynamics should consider Ca^{2+} homeostasis in the junctional and subsarcolemmal spaces, cytosol and mitochondria.

[4] In agreement with the working hypothesis, depending on the fraction of mitochondria interacting with the cytosolic region of high Ca^{2+} concentration, there is an important modification on the whole Ca^{2+} dynamics, although there is almost no effect on the cardiac action potential. This fact supports the key role of mitochondria in determining the Ca^{2+} dynamics in cardiomyocytes, and in the same vein, the findings presented point out the crucial role of spatial aspects to explain controversial results.

Conclusiones

[1] Los sitemas biológicos tales como los cardiomiocitos Biological systems as *cardiomyocytes* are characterized by their complexity leading to highly stiff mathematical models. Then special numerical methods as backward differentiation formula are necessary to solve them.

[2] A very useful approach to simulate steep concentration gradients of microdomains is the called Common-Pool method, which is actually a compartmental modelling approach. In the biological system studied in this work, it allowed to get a realistic description of the dyadic cleft and the subsarcolemmal space, which are characterized by containing large amounts of Ca^{2+} in a very small space.

[3] The problem of simulating the spatial Ca^{2+} dynamics of *cardiomyocytes* can be addressed by compartmental modelling. Thereby, a compartmental model able to reproduce Ca^{2+} dynamics should consider Ca^{2+} homeostasis in the junctional and subsarcolemmal spaces, cytosol and mitochondria.

[4] In agreement with the working hypothesis, depending on the fraction of mitochondria interacting with the cytosolic region of high Ca^{2+} concentration, there is an important modification on the whole Ca^{2+} dynamics, although there is almost no effect on the cardiac action potential. This fact supports the key role of mitochondria in determining the Ca^{2+} dynamics in cardiomyocytes, and in the same vein, the findings presented point out the crucial role of spatial aspects to explain controversial results.

Chapter 6

Research products during the master

[1] Wacquier Benjamin, Romero C. Hugo E., Gonzalez-Velez Virginia, Combettes Laurent and Dupont Geneviève (2017). *Mitochondrial Ca^{2+} dynamics in cells and suspensions*. The FEBS Journal 284, pp. 4128–4142.

[2] Romero C. Hugo E., Olivos S. Edgar, González-Vélez Virginia and Dupont Geneviève (2016). *A model-based investigation of the link between metabolism and electrical activity in pancreatic α-cells*. Poster session at 10^{th} European Conference on Mathematical and Theoretical Biology & SMB Meeting ECMTB2016, Nottingham, UK.

[3] Olivos S. Edgar, Romero C. Hugo E., Dupont Geneviève and Gonzalez-Velez Virginia (2016). *A Model-based Analysis of Glycolytic Oscillations and Electrical Activity in Pancreatic Alpha-cells*. Biomath Communications, Vol. 3, No. 1, pp.52.

Appendix A

Parameters of Wacquier's mitochondrial model

TABLE A.1: Meaning and value of WM parameters.

Parameter	Definition	Value	Reference
a_1	Scaling factor between NADH consumption and change in membrane voltage	20	Wacquier et al., 2016
a_2	Scaling factor between ATP production by ATPase and change in membrane voltage	3.43	Bertram et al., 2006
α	Volumic ratio between the endoplasmic reticulum and the cytosol	0.1	Dupont and Croisier, 2010
α_c	Factor taking cytosolic ADP and ATP buffering into account	0.111	Fall and Keizer, 2001
α_m	Factor taking mitochondrial ADP and ATP buffering into account	0.1391	Fall and Keizer, 2001
AN_{cT}	Total concentration in cytosolic adenine nucleotides	$2500\mu M$	Beis and Newsholme, 1975
AN_{mT}	Total concentration in mitochondrial adenine nucleotides	$15000\mu M$	Bertram et al., 2006
b	Ca^{2+} leak from the endoplasmic reticulum	0.01	Wacquier et al., 2016
C_p	Mitochondrial inner membrane capacitance divided by F	$1.8\frac{\mu M}{mV}$	Bertram et al., 2006
δ	Volumic ratio between the mitochondria and the cytosol	0.0733	Bertram et al., 2006
F	Faraday constant	$96480\frac{C}{mol}$	NA
f_c	Fraction of free over buffer-bound Ca^{2+} in the cytosol	0.01	Fall and Keizer, 2001
f_r	Fraction of free over buffer-bound Ca^{2+} in the endoplasmic reticulum	0.01	Fall and Keizer, 2001
f_m	Fraction of free over buffer-bound Ca^{2+} in mitochondria	0.0003	Fall and Keizer, 2001
k_1	Rate constant of the Ca^{2+} flux through IP_3R	$30/s$	Wacquier et al., 2016

Continue

Table A.1: Meaning and value of WM parameters.

Parameter	Definition	Value	Reference
K_1	Dissociation constant for Ca^{2+} translocation by the MCU	$6\mu M$	Wacquier et al., 2016
K_2	Dissociation constant for MCU activation by Ca^{2+}	$0.38\mu M$	Magnus and Keizer, 1997
K_a	Dissociation constant of Ca^{2+} from the activating site of the IP_3R	$0.3\mu M$	Swillens, Combettes, and Champeil, 1994
K_{AGC}	Dissociation constant of Ca^{2+} from AGC	$0.14\mu M$	Contreras et al., 2007
K_e	Dissociation constant of ATP from SERCA pumps	$0.05\mu M$	Lytton et al., 1992
k_{GLY}	Velocity of glycolysis (empirical)	$450\frac{\mu M}{s}$	Bertram et al., 2006
K_h	Michaelis-Menten constant for ATP hydrolysis	$1000\mu M$	Wacquier et al., 2016
k_{HYD}	Maximal rate of ATP hydrolysis	$100\frac{\mu M}{s}$	Wacquier et al., 2016
K_i	Dissociation constant of IP_3 binding from its receptor	$1\mu M$	Tran Van Nhieu et al., 2013
k_-	Rate constant of Ca^{2+} dissociation from the inactivating site of the IP_3R	$0.02/s$	Swillens, Combettes, and Champeil, 1994
k_o	Rate constant of NADH oxidation by ETC	$600\frac{\mu M}{s}$	Bertram et al., 2006
K_p	Dissociation constant of Ca^{2+} from SERCA receptor	$0.35\mu M$	Tran Van Nhieu et al., 2013
k_+	Rate constant of Ca^{2+} binding to the inhibiting site of the IP_3R	$20\frac{1}{\mu M^4 \cdot s}$	Wacquier et al., 2016
k_x	Rate constant of bidirectional Ca^{2+} leak from mitochondria	$0.008/s$	Wacquier et al., 2016
L	Allosteric equilibrium constant for uniporter conformations	50	Magnus and Keizer, 1998
n_a	Hill coefficient of Ca^{2+} binding to the activating site of the IP_3R	3.5	Swillens, Combettes, and Champeil, 1994
NAD_T	Total concentration of mitochondrial pyridine nucleotides	$250\mu M$	Wacquier et al., 2016
n_i	Hill coefficient of Ca^{2+} binding to the inhibiting site of the IP_3R	4	Swillens, Combettes, and Champeil, 1994
p_1	Voltage dependence coefficient of MCU activity	$0.1/mV$	Wacquier et al., 2016
p_2	Voltage dependence coefficient of NCX activity	$0.016/mV$	Wacquier et al., 2016
p_3	Voltage dependence coefficient of calcium leak	$0.05/mV$	Wacquier et al., 2016
p_4	Voltage dependence coefficient of AGC activity	$0.01/mV$	Wacquier et al., 2016
q_1	Michaelis-Menten-like constant for NAD^+ consumption by the Krebs cycle	1	Bertram et al., 2006

Continue

Table A.1: Meaning and value of WM parameters.

Parameter	Definition	Value	Reference
q_2	$S_{0.5}$ value for activation the Krebs cycle by Ca^{2+}	$0.1\mu M$	Wacquier et al., 2016
q_x	$S_{0.5}$ value for value for indirect inhibition of the AGC by cytosolic Ca^{2+}	$0.1\mu M$	Wacquier et al., 2016
q_3	Michaelis-Menten constant for NADH consumption by the ETC	$100\mu M$	Bertram et al., 2006
q_4	Voltage dependence coefficient 1 of ETC activity	$177mV$	Bertram et al., 2006
q_5	Voltage dependence coefficient 2 of ETC activity	$5mV$	Bertram et al., 2006
q_6	Inhibition constant of ATP_{ase} activity by ATP	$10000\mu M$	Bertram et al., 2006
q_7	Voltage dependence coefficient of ATP_{ase} activity	$190mV$	Bertram et al., 2006
q_8	Voltage dependence coefficient of ATP_{ase} activity	$8.5mV$	Bertram et al., 2006
q_9	Voltage dependence of the proton leak	$2\frac{\mu M}{s\cdot mV}$	Bertram et al., 2006
q_{10}	Rate constant of the voltage-independent proton leak	$-30\frac{\mu M}{s}$	Bertram et al., 2006
R	Perfect gas constant	$8315\frac{mJ}{mol\cdot K}$	NA
T	Temperature	$310.16K$	NA
V_{ANT}	Rate constant of the adenine nucleotide translocator	$5000\frac{\mu M}{s}$	Bertram et al., 2006
V_{AGC}	Rate constant of NADH production via malate-aspartate shuttle	$25\frac{\mu M}{s}$	Wacquier et al., 2016
$V_{F_1F_o}$	Rate constant of the F_1F_o ATP_{ase}	$35000\frac{\mu M}{s}$	Bertram et al., 2006
V_{MCU}	Rate constant of the MCU	$0.0006\frac{\mu M}{s}$	Wacquier et al., 2016
V_{NCX}	Rate constant of the NCX	$0.35\frac{\mu M}{s}$	Wacquier et al., 2016
V_p	Rate constant of the SERCA pumps	$120\frac{\mu M}{s}$	Tran Van Nhieu et al., 2013
C_T	Total concentration of Ca^{2+} in the cell	$2200\mu M$	Wacquier et al., 2016

TABLE A.2: Kinetic expressions for fluxes and reaction rates of Wacquier et al., 2016 model.

Meaning	Expression	Reference
Flux of Ca^{2+} through the IP_3R, $r \rightarrow c$	$J_{IP3} = k_1(b + IR_a)(Ca_r - Ca_c)$ $IR_a = (1 - R_i)\frac{I^2}{K_I^2+I^2}\frac{Ca_c^{n_a}}{K_a^{n_a}+Ca_c^{n_a}}$	Dupont and Croisier, 2010
Ca^{2+} flux through an unidirectional SERCA ATP_{ase}, $c \rightarrow r$	$J_{SERCA} = V_p\frac{Ca_c^2}{K_p^2+Ca_c^2}\frac{ATP_c}{K_e+ATP_c}$	Lytton et al., 1992
Flux of Ca^{2+} through the MCU*, $c \rightarrow m$	$J_{MCU} = V_{MCU}\frac{\frac{Ca_c}{K_1}\left(1+\frac{Ca_c}{K_1}\right)^3}{\left(1+\frac{Ca_c}{K_1}\right)^4+\frac{L}{\left(1+\frac{Ca_c}{K_2}\right)^{2.8}}}e^{p_1V_m}$	Magnus and Keizer, 1997
Rate of Ca^{2+} extrusion by the Na^+/Ca^{2+} exchanger, $m \rightarrow c$	$J_{NCX} = V_{NCX}(\frac{Ca_m}{Ca_c})e^{p_2V_m}$	Bertram et al., 2006
Bidirectional Ca^{2+} flux between mitochondria and cytosol, $c \leftrightarrow m$	$J_x = k_x(Ca_c - Ca_m)e^{p_3V_m}$	Wacquier et al., 2016
Rate of PDH†-catalysed reaction plus glycolysis and Krebs cycle	$J_{PDH} = k_{GLY}\frac{1}{q_1+\frac{NADH}{NAD_T}}\frac{Ca_m}{q_2+Ca_m}$	Bertram et al., 2006
Electrogenic aspartate-glutamate carrier	$J_{AGC} = V_{AGC}\frac{Ca_c}{K_{AGC}+Ca_c}\frac{q_x}{q_x+Ca_c}e^{p_4V_m}$	Wacquier et al., 2016
Rate of NADH oxidation and H^+ extrusion	$J_O = k_o\frac{NADH}{q_3+NADH}\left(1+e^{\frac{V_m-q_4}{q_5}}\right)^{-1}$	Bertram et al., 2006; Wacquier et al., 2016
ATP-ADP translocator	$J_{ANT} = V_{ANT}\frac{1-\frac{\alpha_c ATP_c ADP_m}{\alpha_m ADP_c ATP_m}e^{-\frac{FV_m}{RT}}}{\left(1+\alpha_c\frac{ATP_c}{ADP_c}e^{-0.5\frac{FV_m}{RT}}\right)\left(1+\frac{ADP_m}{\alpha_m ATP_m}\right)}$	Magnus and Keizer, 1997
Rate of ATP synthesis by the F_1F_o-ATP_{ase}	$J_{F_1F_o} = V_{F_1F_o}\left(\frac{q_6}{q_6+ATP_m}\right)\left(1+e^{\frac{q_7-V_m}{q_8}}\right)^{-1}$	Bertram et al., 2006
ATP consumption in cytosol	$J_{HYD} = \frac{J_{SERCA}}{2} + k_{HYD}\frac{ATP_c}{ATP_c+K_h}$	Wacquier et al., 2016
Ohmic mitochondrial proton leak	$J_{Hleak} = q_9V_m + q_{10}$	Bertram et al., 2006

*Mitochondrial Ca^{2+} Uniporter, †Pyruvate Dehydrogenase.

Appendix B

Stiffness of differential equation systems

An ordinary differential equations problem is stiff if its numerical solution is smooth and is varying slowly in the time interval of computation, but there are nearby solution curves varying much more rapidly (LeVeque, 2008). In other words, stiffness arises when some components of the solution decay more rapidly than others, and so a very small step size is necessary to get stability when integrating the system (Alberdi, 2014).

Stiffness is very common in cellular systems due to the very different timescales at which processes occur (Gillespie and Petzold, 2006; Rihan, 2013). It is worth mention that when solving a stiff problem, it is possible to use explicit methods, as Euler explicit method, however, it is very costly in computational terms because of the necessity to restrict the step size based on the fastest component, which is in fact due to the step size-dependent stability of that kind of methods (Gillespie and Petzold, 2006).

Implicit methods are stable, so they are used to overcome the limitations of explicit methods and result much more efficient for solving stiff systems. In this work, all systems of differential equations are stiff since timescales of some components are quite different (see Figure 2.4), so an implicit method named Backward Differentiation Formulae was used for its intergration (Alberdi, 2014; Gillespie and Petzold, 2006).

Appendix C

An equation for MCU flux in cardiac mitochondria

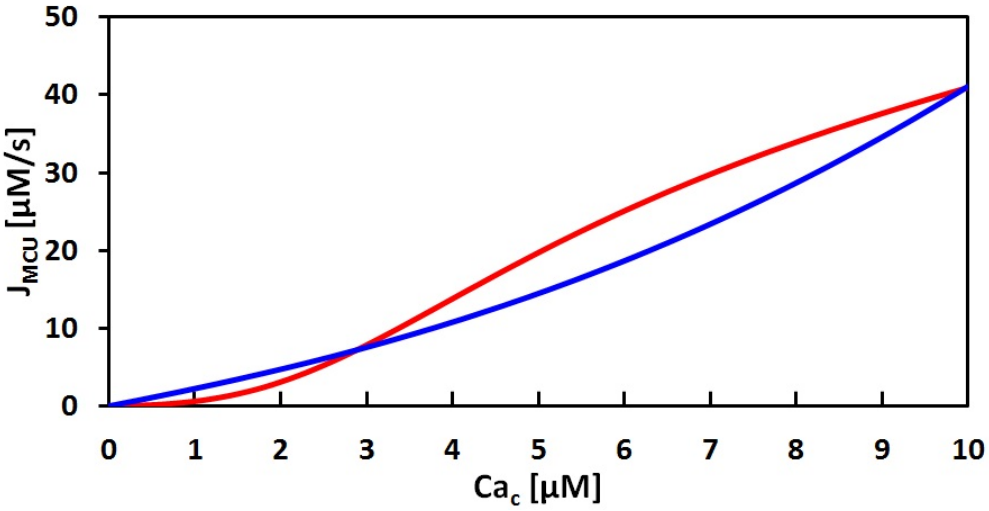

FIGURE C.1: Flux through MCU depending on cytosolic Ca^{2+}. Red: Equation of WM ($K_1 = 21\mu M$, $K_2 = 1.33\mu M$, $V_{MCU} = 1.5 \cdot 10^{-5} \frac{\mu M}{s}$). Blue: Equation proposed by Williams et al., 2013. This latter fits to several experimental data. In both cases the membrane potential is fixed at 160mV.

TABLE C.1: MCU flux equation of Williams et al., 2013.

Variable	Equation	Number
Flux of Ca^{2+} through the MCU	$J_{MCU} = Po \cdot N_{mito} \cdot N_{MCU} \frac{i_{MCU}}{z \cdot F \cdot V_c}$	(B.1)
Single MCU-channel current	$i_{MCU} = g_{MCU}(V_m - E_{Ca^{2+}})$	(B.2)
Open probability of MCU	$Po = Po_{min} + (Po_{max} - Po_{min}) \frac{Ca_c^{\eta}}{K_{mPo}^{\eta} + Ca_c^{\eta}}$	(B.3)

$N_{mito} = 10000$, number of mitochondria per cell ;$N_{MCU} = 200$, number of MCU per mitochondria; $z = 2$, valency of Ca2+; F Faraday's constant; $Vc = 18 \cdot 10^{-6} \mu L$, cytosolic volume of *myocytes*; $g_{MCU} = 8.1pS$, single channel MCU conductance; $E_{Ca^{2+}} = -135mV$, Nernst reversal potential for Ca^{2+}; $\eta = 1.45$, cooperativity factor for activation, $K_{mPo} = 19000 \mu M$, Michaelis–Menten constant; $Po_{min} = 0.03$ and $Po_{max} = 0.9$.

Bibliography

Alberdi, Elisabete Celaya (2014). "Métodos numéricos para ecuaciones diferenciales rígidas. Aplicación a la semidiscretización del Método de Elementos Finitos." PhD thesis. Universidad del País Vasco, p. 295.

Amundson, Jeffrey and David E. Clapham (1993). "Calcium waves". In: *Current Opinion in Neurobiology* 3.3, pp. 375–382. ISSN: 09594388. DOI: 10.1016/0959-4388(93)90131-H.

Babcock, Donner F. et al. (1997). "Mitochondrial participation in the intracellular Ca2+ network". In: *Journal of Cell Biology* 136.4, pp. 833–844. ISSN: 00219525. DOI: 10.1083/jcb.136.4.833.

Bakker, Jacques M.T. and Harold V.M. van Rijen (2010). "Cardiac Action Potentials, Ion Channels, and Gap Junctions". In: *Cardiac Electrophysiology Methods and Models*, pp. 53–72. ISBN: 9781441966575. DOI: 10.1007/978-1-4419-6658-2.

Barnett, V. A. (2005). "Cardiac Myocytes". In: *Handbook of Cardiac Anatomy, Physiology, and Devices*. New Jersey: Humana Press Inc. Chap. 8, pp. 113–121.

Bassingthwaighte, James B et al. (2012). "Compartmental modeling in the analysis of biological systems." In: *Methods in molecular biology* 929, pp. 391–438. ISSN: 1940-6029. DOI: 10.1007/978-1-62703-050-2_17.

Baughman, Joshua M. et al. (2011). "Integrative genomics identifies MCU as an essential component of the mitochondrial calcium uniporter". In: *Nature* 476.7360, pp. 341–345. ISSN: 00280836. DOI: 10.1038/nature10234. arXiv: NIHMS150003.

Bazil, Jason N and Ranjan K Dash (2011). "A minimal model for the mitochondrial rapid mode of Ca^{2}+ uptake mechanism." In: *PloS one* 6.6, e21324. ISSN: 1932-6203. DOI: 10.1371/journal.pone.0021324.

Beis, I and E A Newsholme (1975). "The contents of adenine nucleotides, phosphagens and some glycolytic intermediates in resting muscles from vertebrates and invertebrates." In: *The Biochemical journal* 152.1, pp. 23–32. ISSN: 0264-6021. DOI: 10.1042/bj1520023.

Bernardi, Paolo and Fabio Di Lisa (2015). *The mitochondrial permeability transition pore: Molecular nature and role as a target in cardioprotection*. DOI: 10.1016/j.yjmcc.2014.09.023.

Bers, Donald M (2002). "Cardiac excitation-contraction coupling." In: *Nature* 415.6868, pp. 198–205. ISSN: 0028-0836. DOI: 10.1038/415198a.

Bers, Donald M. (2008). "Calcium cycling and signaling in cardiac myocytes." In: *Annual review of physiology* 70, pp. 23–49. ISSN: 0066-4278. DOI: 10.1146/annurev.physiol.70.113006.100455.

Bertram, Richard et al. (2006). "A simplified model for mitochondrial ATP production". In: *Journal of Theoretical Biology* 243.4, pp. 575–586. ISSN: 00225193. DOI: 10.1016/j.jtbi.2006.07.019.

Beutner, Gisela et al. (2005). "Type 1 ryanodine receptor in cardiac mitochondria: Transducer of excitation-metabolism coupling". In: *Biochimica et Biophysica Acta - Biomembranes* 1717.1, pp. 1–10. ISSN: 00052736. DOI: 10.1016/j.bbamem.2005.09.016.

Blaustein, M. P. (1985). "Intracellular Calcium as a Second Messenger, What's so Special about Calcium?" In: *Calcium in Biológical Sistems*. New York: Plenum Press. Chap. 3, pp. 23–33. ISBN: 978-1-4613-2377-8. DOI: 10.1007/978-1-4613-2377-8_3.

Bootman, M D, P Lipp, and M J Berridge (2001). "The organisation and functions of local Ca(2+) signals." In: *Journal of cell science* 114.Pt 12, pp. 2213–2222. ISSN: 0021-9533. DOI: 10.1085/jgp.116.5.697.

Boyman, Liron et al. (2014). "Calcium movement in cardiac mitochondria". In: *Biophysical Journal* 107.6, pp. 1289–1301. ISSN: 15420086. DOI: 10.1016/j.bpj.2014.07.045.

Buntinas, Linas et al. (2001). "The rapid mode of calcium uptake into heart mitochondria (RaM): Comparison to RaM in liver mitochondria". In: *Biochimica et Biophysica Acta- Bioenergetics* 1504.2-3, pp. 248–261. ISSN: 00052728. DOI: 10.1016/S0005-2728(00)00254-1.

Conrad, E. D. and J. J. Tyson (2006). "Modeling Molecular Interaction Networks with Nonlinear Ordinary Differential Equations". In: *System Modeling in Cell Biology*. Massachusetts: MIT Press. Chap. 6, pp. 97–123.

Contreras, Laura et al. (2007). "Ca2+ activation kinetics of the two aspartate-glutamate mitochondrial carriers, aralar and citrin: Role in the heart malate-aspartate NADH shuttle". In: *Journal of Biological Chemistry* 282.10, pp. 7098–7106. ISSN: 00219258. DOI: 10.1074/jbc.M610491200.

Cortassa, Sonia et al. (2003). "An integrated model of cardiac mitochondrial energy metabolism and calcium dynamics". In: *Biophysical Journal* 84.4, pp. 2734–2755. ISSN: 00063495. DOI: 10.1016/S0006-3495(03)75079-6.

De Marchi, Umberto et al. (2014). "NCLX protein, but not LETM1, mediates mitochondrial Ca2+ extrusion, thereby limiting Ca2+-induced NAD(P)H production and modulating matrix redox state". In: *Journal of Biological Chemistry* 289.29, pp. 20377–20385. ISSN: 1083351X. DOI: 10.1074/jbc.M113.540898.

Dedkova, Elena N. and Lothar A. Blatter (2008). *Mitochondrial Ca2+ and the heart*. DOI: 10.1016/j.ceca.2007.11.002.

— (2013). *Calcium signaling in cardiac mitochondria*. DOI: 10.1016/j.yjmcc.2012.12.021. arXiv: NIHMS150003.

Denton, Richard M. (2009). *Regulation of mitochondrial dehydrogenases by calcium ions*. DOI: 10.1016/j.bbabio.2009.01.005.

Dupont, Geneviève and Huguette Croisier (2010). "Spatiotemporal organization of Ca dynamics: a modeling-based approach." In: *HFSP journal* 4.2, pp. 43–51. ISSN: 1955-205X. DOI: 10.2976/1.3385660.

Dupont, Geneviève et al. (2016). *Models of Calcium Signalling*. Switzerland: Springer International Publishing, pp. XXIII, 436. ISBN: 978-3-319-29645-6. DOI: 10.1007/978-3-319-29647-0.

Enderle, John D. (2011). "Compartmental Modeling". In: *Introduction to Biomedical Engineering*, pp. 359–445. ISBN: 9780123749796. DOI: 10.1016/B978-0-12-374979-6.00007-1.

Fall, C P and J E Keizer (2001). *Mitochondrial modulation of intracellular Ca(2+) signaling*. DOI: 10.1006/jtbi.2000.2292.

Fedrizzi, Laura, Dmitry Lim, and Ernesto Carafoli (2008). "Calcium and signal transduction." In: *Biochemistry and molecular biology education : a bimonthly publication of the International Union of Biochemistry and Molecular Biology* 36.3, pp. 175–180. ISSN: 1470-8175. DOI: 10.1002/bmb.20187.

Fieni, Francesca et al. (2012). "Activity of the mitochondrial calcium uniporter varies greatly between tissues". In: *Nature Communications* 3. ISSN: 20411723. DOI: 10.1038/ncomms2325.

Gillespie, Daniel; and Linda. Petzold (2006). "System Modeling in Cell Biology". In: *System Modeling in Cell Biology From Concepts to Nuts and Bolts*. Massachusetts Institute of Technology. Chap. 16, pp. 331–354.

Goldbeter, Albert, Genevie've Dupont, and Michael J. Berridge (1990). "Minimal model for signal-induced Ca2+ oscillations and for their frequency encoding through protein phosphorylation." In: *Proceedings of the National Academy of Sciences of the United States of America* 87.4, pp. 1461–1465. ISSN: 0027-8424. DOI: 10.1073/pnas.87.4.1461.

Grandi, Eleonora, Francesco S. Pasqualini, and Donald M. Bers (2010). "A novel computational model of the human ventricular action potential and Ca transient". In: *Journal of Molecular and Cellular Cardiology* 48.1, pp. 112–121. ISSN: 00222828. DOI: 10.1016/j.yjmcc.2009.09.019. arXiv: NIHMS150003.

Griffiths, Elinor J. and Guy A. Rutter (2009). "Mitochondrial calcium as a key regulator of mitochondrial ATP production in mammalian cells". In: *Biochimica et Biophysica Acta (BBA) - Bioenergetics* 1787.11, pp. 1324–1333. ISSN: 0005-2728. DOI: 10.1016/j.bbabio.2009.01.019.

Hake, Johan and Glenn T Lines (2008). "Stochastic binding of Ca2+ ions in the dyadic cleft; continuous versus random walk description of diffusion." In: *Biophysical journal* 94.11, pp. 4184–201. ISSN: 1542-0086. DOI: 10.1529/biophysj.106.103523.

Ichas, François and Jean Pierre Mazat (1998). *From calcium signaling to cell death: Two conformations for the mitochondrial permeability transition pore. Switching from low- to high-conductance state*. DOI: 10.1016/S0005-2728(98)00119-4.

Ishii, Kiyoaki, Kenzo Hirose, and Masamitsu Iino (2006). "Ca2+ shuttling between endoplasmic reticulum and mitochondria underlying Ca2+ oscillations". In: *EMBO Reports* 7.4, pp. 390–396. ISSN: 1469221X. DOI: 10.1038/sj.embor.7400620. arXiv: /www.pubmedcentral.nih.gov/articlerender.fcgi?artid=3006164{\&}tool=pmcentrez{\&}rendertype=abstract. [Figures, S., 2010. Supplementary information. Nature, 1(c), pp.1–7. Available at: http:].

Keener, J. and J. Keizer (2002). "Spatial Modeling". In: *Computational Cell Biology*. New York: Springer Science+Business Media. Chap. 7, pp. 171–197.

Keener, James P and James Sneyd (2008). "Mathematical Physiology I: Cellular Physiology". In: *Book*, p. 580. ISSN: 9780387877075. DOI: 10.1007/978-0-387-79388-7. arXiv: 1406.6401.

Kell, D. B. and J. D. Knowles (2006). "The Role of Modeling in Systems Biology". In: *System Modeling in Cell Biology*. Massachusetts: MIT Press. Chap. 1, pp. 3–18.

Klabunde, R. E. (2007). *Cardiac Myocytes and Sarcomeres*.

Kohlhaas, Michael and Christoph Maack (2013). *Calcium release microdomains and mitochondria*. DOI: 10.1093/cvr/cvt032.

Laske, T. G. and P. A. Iaizzo (2005). "The Cardiac Conduction System". In: *Handbook of Cardiac Anatomy, Physiology, and Devices*. New Jersey: Humana Press Inc. Chap. 9, pp. 123–136.

LeVeque, R J (2008). *Finite Difference Methods for Ordinary and Partial Differential Equations*, pp. 1–356. ISBN: 9780898716290. DOI: 10.1137/1.9780898717839.

Lytton, Jonathan et al. (1992). *Functional comparisons between isoforms of the sarcoplasmic or endoplasmic reticulum family of calcium pumps*.

Maack, Christoph and Brian O'Rourke (2007). *Excitation-contraction coupling and mitochondrial energetics*. DOI: 10.1007/s00395-007-0666-z. arXiv: NIHMS150003.

Magnus, G and J Keizer (1997). "Minimal model of beta-cell mitochondrial Ca2+ handling." In: *The American journal of physiology* 273.2 Pt 1, pp. C717–33. ISSN: 0002-9513.

— (1998). "Model of beta-cell mitochondrial calcium handling and electrical activity. I. Cytoplasmic variables." In: *The American journal of physiology* 274, pp. C1158–C1173. ISSN: 0002-9513.

O'Rourke, Brian and Lothar A. Blatter (2009). "Mitochondrial Ca2+ uptake: Tortoise or hare?" In: *Journal of Molecular and Cellular Cardiology* 46.6, pp. 767–774. ISSN: 00222828. DOI: 10.1016/j.yjmcc.2008.12.011. arXiv: NIHMS150003.

Paillard, Melanie et al. (2017). "Tissue-Specific Mitochondrial Decoding of Cytoplasmic Ca2+Signals Is Controlled by the Stoichiometry of MICU1/2 and MCU". In: *Cell Reports* 18.10, pp. 2291–2300. ISSN: 22111247. DOI: 10.1016/j.celrep.2017.02.032.

Palmer, Amy E. et al. (2006). "Ca2+ Indicators Based on Computationally Redesigned Calmodulin-Peptide Pairs". In: *Chemistry and Biology* 13.5, pp. 521–530. ISSN: 10745521. DOI: 10.1016/j.chembiol.2006.03.007.

Ridgway, Douglas, Gordon Broderick, and Michael J. Ellison (2006). *Accommodating space, time and randomness in network simulation*. DOI: 10.1016/j.copbio.2006.08.004.

Rihan, Fathalla A. (2013). "Numerical modeling of fractional-order biological systems". In: *Abstract and Applied Analysis* 2013. ISSN: 10853375. DOI: 10.1155/2013/816803.

Rizzuto, Rosario et al. (2012). "Mitochondria as sensors and regulators of calcium signalling". In: *Nature Reviews Molecular Cell Biology* 13.9, pp. 566–578. ISSN: 1471-0072. DOI: 10.1038/nrm3412. arXiv: NIHMS150003.

Ryu, Shin Young et al. (2010). *Mitochondrial ryanodine receptors and other mitochondrial Ca2+ permeable channels*. DOI: 10.1016/j.febslet.2010.01.032. arXiv: NIHMS150003.

Sedova, Marina, Elena N Dedkova, and Lothar A Blatter (2006). "Integration of rapid cytosolic Ca2+ signals by mitochondria in cat ventricular myocytes". In: *American journal of physiology. Cell physiology* 291, pp. 840–850. ISSN: 0363-6143. DOI: 10.1152/ajpcell.00619.2005..

Shannon, T R et al. (2004). "A mathematical treatment of integrated Ca dynamics within the ventricular myocyte". In: *Biophys. J* 87.November, pp. 3351–3371. ISSN: 0006-3495. DOI: 10.1529/biophysj.104.047449.

Swillens, S, L Combettes, and P Champeil (1994). "Transient inositol 1,4,5-trisphosphate-induced Ca2+ release: a model based on regulatory Ca(2+)-binding sites along the permeation pathway." In: *Proceedings of the National Academy of Sciences of the United States of America* 91.21, pp. 10074–10078. ISSN: 0027-8424. DOI: 10.1073/pnas.91.21.10074.

Szabadkai, G and M R Duchen (2008). "Mitochondria: the hub of cellular Ca2+ signaling". In: *Physiology (Bethesda)* 23, pp. 84–94. ISSN: 1548-9213. DOI: 10.1152/physiol.00046.2007.

Szallasi, Zoltan, J. Stelling, and V. Periwal (2006). *System Modeling in Cellular Biology*. Vol. System Mod, p. 452. ISBN: 0262195488. DOI: 10.7551/mitpress/9780262195485.001.0001.

Tarasov, Andrei I., Elinor J. Griffiths, and Guy A. Rutter (2012). "Regulation of ATP production by mitochondrial Ca2+". In: *Cell Calcium* 52.1, pp. 28–35. ISSN: 01434160. DOI: 10.1016/j.ceca.2012.03.003.

Thul, R. et al. (2008). "Calcium Oscillations". In: *Cellular Oscillatory Mechanisms*. New York: Springer Science+Business Media. Chap. 1, pp. 1–27.

Thul, R. et al. (2015). "Unifying principles of calcium wave propagation - Insights from a three-dimensional model for atrial myocytes". In: *Biochimica et Biophysica Acta - Molecular Cell Research* 1853.9, pp. 2131–2143. ISSN: 18792596. DOI: 10.1016/j.bbamcr.2015.02.019.

Tran Van Nhieu, Guy et al. (2013). "Actin-based confinement of calcium responses during Shigella invasion". In: *Nature Communications* 4. ISSN: 20411723. DOI: 10.1038/ncomms2561.

Wacquier, Benjamin et al. (2016). "Interplay Between Intracellular Ca2+ Oscillations and Ca2+-stimulated Mitochondrial Metabolism". In: *Scientific reports* 6.19316, pp. 1–16. DOI: 10.1038/srep19316.

Wacquier, Benjamin et al. (2017). "Mitochondrial Ca 2+ dynamics in cells and suspensions". In: *The FEBS Journal* 284, pp. 4128–4142. ISSN: 1742464X. DOI: 10.1111/febs.14296.

Williams, George S B et al. (2013). "Mitochondrial calcium uptake." In: *Proceedings of the National Academy of Sciences of the United States of America* 110.26, pp. 10479–86. ISSN: 1091-6490. DOI: 10.1073/pnas.1300410110.

Winslow, Raimond L. et al. (2011). "Integrative modeling of the cardiac ventricular myocyte". In: *Wiley Interdisciplinary Reviews: Systems Biology and Medicine* 3.4, pp. 392–413. ISSN: 19395094. DOI: 10.1002/wsbm.122.

Wolkenhauer, Olaf (2014). "Why model?" In: *Frontiers in Physiology* 5 JAN. ISSN: 1664042X. DOI: 10.3389/fphys.2014.00021.